JPEG2000 Image Transmission over Frequency Selective Channels

by

Moein Shayegannia

B.Sc., American University of Sharjah, 2008

Thesis Submitted in Partial Fulfillment
of the Requirements for the Degree of
Master of Applied Science

in the
School of Engineering Science
Faculty of Applied Sciences

SIMON FRASER UNIVERSITY

Fall 2012

Approval

Name: **Moein Shayegannia**

Degree: **Master of Applied Science**

Title of Thesis: ***JPEG2000 Image Transmission over Frequency Selective Channels***

Examining Committee:

Chair: Dr. John Jones
Associate Professor & Acting Director, School of Engineering Science

---

Dr. Sami Muhaidat
Senior Supervisor
Assistant Professor, School of Engineering Science

Dr. Atousa Hajshirmohammadi
Co-Supervisor
Senior Lecturer, School of Engineering Science

Dr. Jie Liang
Internal Examiner
Associate Professor, School of Engineering Science

Date Defended/Approved: August 27, 2012

Partial Copyright License

Abstract

This thesis addresses transmission of JPEG2000 coded images over frequency selective channels. We utilize an unequal power allocation algorithm to protect the codestream against disturbances in the wireless fading channel. To eliminate the negative effects of inter symbol interference and inter carrier interference, we design two separate systems for downlink and uplink data transmission: an orthogonal frequency division multiplexing system (downlink) and a single carrier frequency domain equalization system (uplink). We also investigate the time complexity of the power allocation algorithm, and assess the optimization process for minimizing the end to end distortion of the received images. The performance of our systems is further analyzed under deployment of multiple transmitter antennas, to achieve spatial diversity by incorporating space time block coding technique into the transmitter model. In addition, we explore addition of a linear constellation pre-coder matrix to the OFDM system to achieve multipath diversity during transmission of JPEG2000 images. The simulation results demonstrate a performance evaluation of our proposed systems for JPEG2000 image transmission with competing strategies, and measure transmission bandwidth efficiency and peak signal to noise ratio profile of the received images in our proposed systems.

Keywords: JPEG2000; Frequency Selective Channel; Unequal Power Allocation; Orthogonal Frequency Division Multiplexing; Single Carrier Frequency Domain Equalization

Dedication

To My beloved Parents and sister

Acknowledgements

First and foremost, my utmost gratitude goes to Allah, God Almighty, who gave me the strength and the blessing to accomplish my master work.

I am cordially grateful to my senior supervisor, Dr. Sami Muhaidat, and my supervisor, Dr. Atousa Hajshirmohammadi. It was their guidance, consistent support, and patience with my mistakes that led me develop the required skills in these years to understand the subject and tackle its issues.

I would also like to thank Dr. Jie Liang for serving as my examiner and guiding me anytime I had questions, Dr. Paul Ho for his supports during these years, and Dr. Rodney Vaughen for all of technical supports and lovely conversations in these years. I would like to extend my gratefulness to Dr. John Jones for his time and energy as my session defence chair.

I am forever indebted to my lovely parents and sister, without their endless love, support, and wisdom I would have never achieved my goals. I would like to also thank all the graduate students in the wireless communication laboratory at Simon Fraser University, in particular, Saeid, Alireza, Milad, Mehdi, Maral, Ehsan, Hamidreza, Hossein, Ali, Amin, Homa, Mahsa, Babak, and Omar. They have been my true friends during these years and have shared with me many technical experiences and those that I will carry with me in life. I would also like to thank Mahin Torki for her technical guidance to my research project.

Table of Contents

List of Tables

List of Figures

Acronyms

AWGN	Additive White Gaussian Noise
BER	Bit Error Rate
BPSK	Binary Phase Shift Keying
CB	Code Block
CIR	Channel Impulse Response
CP	Coding Pass
CP-SC	Cyclic Prefixed-Single Carrier
CSI	Channel State Information
DAB	Digital Audio Broadcasting
DVB-T	Digital Video Broadcasting-Terrestrial
DWT	Discrete Wavelet Transform
EPA	Equal Power Allocation
FEC	Forward Error Correction
FFT	Fast Fourier Transform
FMRI	Functional Magnetic Resonance Imaging
HDSL	High-bit-rate Digital Subcarrier Line
ICI	Inter Carrier Interference
IFFT	Inverse Fast Fourier Transform
ISI	Inter Symbol Interference
LCP	Linear Constellation Pre-coding
MMSE	Minimum Mean Square Error
MSB	Most Significant Bit
MSE	Mean Square Error
OFDM	Orthogonal Frequency Domain Multiplexing
PAPR	Peak to Average Power Ratio
PSNR	Peak Signal to Noise Ratio
RS	Reed Solomon
SA	Simulated Annealing
SCFDE	Single Carrier Frequency Domain Equalization

SNR	Signal to Noise Ratio
SPIHT	Set Partitioning In Hierarchical Trees
STBC	Space Time Block Coding
UEP	Unequal Error Protection
UPA	Unequal Power Allocation
WLAN	Wireless Local Area Network

1. Chapter 1: Introduction

This chapter introduces the motivation behind this thesis, discuses the contributions of this thesis, and provides a brief overview of the key subjects related to the thesis. Section 1.1 discusses the motivation behind the research on transmission of JPEG2000 images over frequency selective channels. Section 1.2 explains the main contribution of this thesis. Section 1.3 explains the JPEG2000 image coder structure. Section 1.4 introduces some of the protection techniques in the literature for image transmission over wireless channels. Section 1.5 elaborates on the space time block coding technique which is considered in our system design later in the thesis. Finally, Section 1.6 lists the publications resulting from this research.

1.1. Motivation

The increasing demand on wireless image transmission requires high data rate and reliable transfer of multimedia streams over severe channel conditions. However, the hostile behavior of wireless medium and large number of users impose challenges in maintaining a high quality of the received images, conserving the available bandwidth, and preserving the total power for transmission. In addition, applications such as medical imagery require not only high quality of the reconstructed images, but also fast coding, delivery, and decoding of these images. To address these challenges, we need to alleviate the sources of disturbance in wireless channels, such as fading, interference, shadowing, path loss, and multipath, by providing techniques which can adapt to different channel conditions, while keeping the complexity of the system low.

To lessen the error impact, it is advantageous to use a source coding technique with some degree of protection against errors. JPEG2000 is one of the recent and advanced source coding techniques for image coding [**1**]. This standard is able to generate an error-resilient and scalable bitstream which allows progressive decoding of the re-

ceived bitstream at different quality and resolution levels. The error resilient tool is able to detect but cannot correct the errors in the code-stream. Once an error is detected within a code block, the data associated with the erroneous coding pass and with the future coding pass of that code block are discarded, and resynchronization mechanism of the received data is performed [**1**]. The JPEG2000 coded bitstream has a hierarchical structure in which some bits hold more important information compared to others, thus it is natural to have higher protection over the more important bits. Different techniques such as Unequal Error Protection (UEP) and Unequal Power Allocation (UPA) are introduced in the literature to enhance the transmission of scalable coded bitstreams. The UEP methods apply Forward Error Correction (FEC) coding with different coding rates to different portions of the bitstream, based on the importance of each portion. The UPA techniques distribute the total available power for transmission of an image unequally over the bitstream in such a way that more power is allocated to the more important bits.

The pioneering works in this area mostly address implementation of the UEP technique to protect images against disturbances in wireless transmission. However, this technique leads to a lower data rate and excessive usage of bandwidth in practice. Recently, focus on protecting images via power allocation techniques for wireless transmission has been increased in the literature. However, most of the available manuscripts have assumed a basic transmission medium of non-frequency selective, which is impractical. Among those that consider frequency selectivity of the channel, a comprehensive investigation on the performance of the UPA or UEP techniques under different transmission scenarios, such as different channel memory lengths, various Signal to Noise Ratio (SNR) values, and multiple transmission antennas has not been analyzed. Furthermore, the literature on transmission of multimedia over frequency selective channels contains employment of the Orthogonal Frequency Division Multiplexing (OFDM) in the transmitter and receiver to combat Inter Symbol Interference (ISI) and Inter Carrier Interference (ICI). Due to the large Peak to Average Power Ratio (PAPR) imposed by the OFDM system, this technique is employed at the base station for down link data transmission. However, for a communication system, exploration of multimedia data transmission in Single Carrier Frequency Domain Equalization (SCFDE) system, which is used to eliminate ISI and ICI in frequency selective channels in the uplink transmission, is mandatory [**2**].

The main purpose of this thesis is to investigate the impact of an optimized UPA technique on the quality of the received JPEG2000 images over wireless channels which suffer from frequency selectivity. We provide Monte-Carlo simulations for different channel memory lengths, on a range of different available SNR values, with single and multiple transmitter antennas. To combat the negative effects of ISI and ICI, we employ the UPA algorithm in an OFDM system for downlink data transmission, and in an SCFDE system for uplink data transmission. We compare the performance of these two systems on the quality of the received images and on the bandwidth efficiency during transmission.

1.2. Main Contributions and Outline

The main contributions of this thesis can be summarized as follow:

Chapter 1 introduces the topic and the motivation behind this research. It also provides a brief review of important background materials related to the thesis. This chapter explains the JPEG2000 Image coder, and elaborates on the structure of this standard. Then, the available protection techniques in the literature for wireless image transmission such as UEP techniques or UPA schemes are discussed. Next, an overview about the Space Time Block Coding (STBC) technique, which is used in this thesis to obtain spatial diversity, is presented.

Chapter 2 explains our proposed OFDM based system model for the downlink transmission of JPEG2000 images with UPA algorithm in broadband networks. This chapter elaborates on the distortion model of the algorithm, the implementation of the UPA algorithm, the time complexity of the algorithm, and modification of the algorithm to compensate for fading in a frequency selective channel. Also an adaptive scheme for the UPA algorithm and a channel assignment strategy for the OFDM transmission are proposed in this chapter. To demonstrate the efficiency of our UPA algorithm in an OFDM based broadband network, a comprehensive Monte Carlo simulation study is provided to examine the Peak Signal to Noise Ratio (PSNR), Bit Error Rate (BER), and visual quality of the received images of the “Lena”, “Peppers”, “Bridge”, and “Couple”, at different sizes and source coding rates.

Chapter 3 describes our proposed SCFDE based system for the uplink transmission of JPEG2000 images with UPA algorithm, in broadband networks. The transmitter and receiver model in the case of single antenna and double antenna at the transmission side is presented. Chapter 3 also covers utilization of the STBC technique in our system model to achieve spatial diversity, and analyzes how to modify the UPA algorithm to adapt a multi-input single-output channel model. The results exhibit the performance of our proposed UPA-SCFDE system in a multi-tap broadband network for wireless image transmission, and present the effectiveness of utilizing multiple antennas at the transmitter on enhancement of the received image quality.

In addition, efficiency of the OFDM and SCFDE systems on transmitting JPEG2000 images over frequency selective channels is compared in Chapter 3. This study is undertaken by comparing the received image quality at different available SNR values, channel memory lengths, bit budget values, and multiple transmission antennas. For the sake of fairness during the comparison, we do not consider any power allocation algorithm, and distribute the available power equally among all the coding passes of the JPEG2000 codestream.

Finally, Chapter 4 concludes the thesis, and provides the possible directions for further research in this field.

1.3. JPEG2000 Structure

The transformation technique used in JPEG2000 is the Discrete Wavelet Transform (DWT). In the JPEG2000 image coder, the first operation is to (optionally) partition a source image into a number of rectangular non-overlapping blocks called tiles. Then DWT is applied to each tile which transforms the samples into spatial frequency subbands at different levels of resolution. The first level of decomposition consists of four subbands LL1, LH1, HL1, HH1 [**3**]. The LL1 subband is the lowest resolution of the tile and is a down-sampled low-resolution representation of the original tile-component. The LL1 subband can be further decomposed by applying DWT. This process can be repeated to obtain different resolution levels. Then, each resolution of each tile component is further partitioned into precincts. Within every subband, each precinct contributes one packet to the code-stream of the image. Precincts are not a partition of image data and

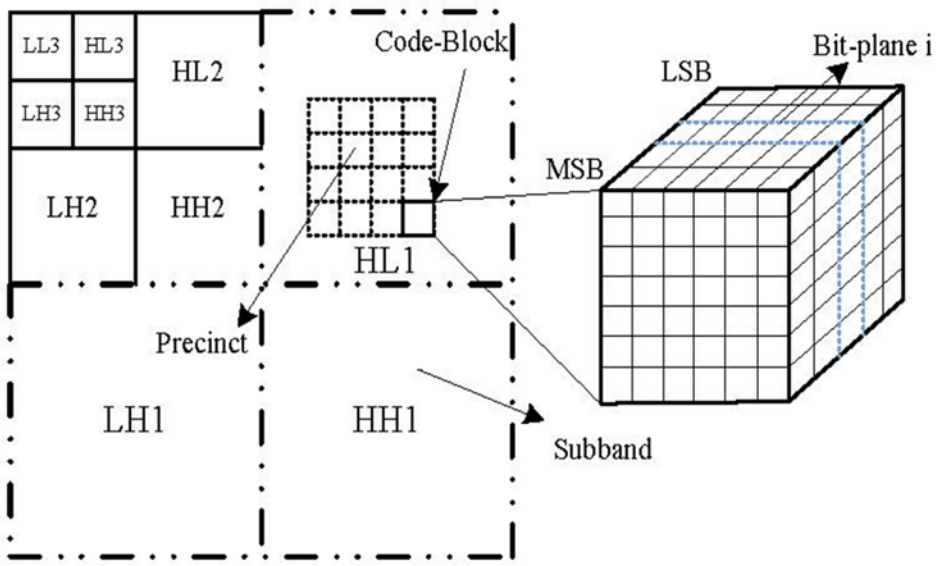

Figure 1-1: Components of a JPEG2000 transformed image

do not impact sample data transformation or coding. Precincts are used to reconstruct the resolution [**4**]. Each subband is partitioned into small blocks, called code-blocks, where quantization and bit-plane coding are initiated. The packets furnished by the precincts identify their header and body from the contributions of the code-blocks belonging to the relevant precinct. Starting from the Most Significant Bit (MSB), the coder scans through the bit-planes of each coding pass within three coding passes. Each of the coding passes collects the relevant information about the bit-plane data. Based on the significance of a particular bit location and its neighboring, location of each bit in the coding passes is decided. The encoder uses this information to generate a compressed bit-stream or a code-stream [**1**]. Figure 1-1 illustrates a 3 layer decomposition of a source image using DWT and its partitioning into four resolution levels, subbands, precincts, and code-blocks. This figure also presents how each code-block is decomposed into a number of bit-planes.

To increase the robustness of the JPEG2000 bitstream against error propagation along the code-stream, error resilient feature is introduced in the standard. Small size code-blocks are independently coded and included with resynchronization markers. As a result, errors do not propagate beyond the code-block whose bit-stream is corrupted, and the markers keep the synchronization between the encoder and decoder in case of

occurrence of bit errors. JPEG2000 standard also provides a mechanism to combine all the packet headers within the main header. This adds an advantage to the decoding process of the received data stream, if the main header can be transmitted in an error-free medium. It is necessary to correctly decode the header of a packet in order to extract the code-block contributions to the body of the packet [**3**], [**1**].

1.4. Overview of Error Protection Techniques for Wireless Image Transmission

Transmission of JPEG2000 images using UEP techniques over slow fading non-frequency selective channels has been widely investigated in [**4**], [**5**], [**6**], and [**7**]. In [**4**], UEP is achieved in JPEG2000 code-streams by using Reed Solomon (RS) block codes. In [**5**], Banister *et al*. make use of Viterbi algorithm to jointly optimize source rate and channel rate for the purpose of UEP. In [**6**], the authors employ product coded streams which consist of Turbo-codes and RS codes to obtain UEP. In [**7**], the authors obtain UEP using RS channel coding for the header and convolutional coding for the body of the image bitstream.

Protection of JPEG2000 images over slow fading non-frequency selective channels using UPA schemes has been reported in [**8**] and [**9**]. Atzori employs an optimized UPA scheme in [**8**] based on increasing JPEG2000 image quality as well as RS channel coding to protect coded bitstream. In [**9**], Torki *et al*. proposes an optimized UPA scheme based on minimizing the total end to end distortion of JPEG2000 images, which proved its effectiveness in improvement of the PSNR performance and at a lower complexity in comparison with the existing UEP techniques.

Evaluation of UEP for JPEG2000 image transmission over frequency selective channels has been investigated in [**10**], [**11**], [**12**], [**13**], [**14**], [**15**], [**16**], [**17**], [**18**], [**19**], [**20**], and [**21**]. Houas *et al*. utilize rate compatible punctured convolutional codes to enable UEP for transmission of the JPEG2000 images in OFDM systems [**10**]. In [**11**], the layer structure of the JPEG2000 is exploited by protecting the data in top layer with an FEC code, and the performance is analyzed in an OFDM transmission system for different channel delays. In [**12**], authors achieve UEP using an optimal joint source-channel coding and consider progressive image transmission over differentially space-time cod-

ed OFDM system. Sethakaset *et al*. propose an UEP scheme in the spatial domain through enhanced beamforming algorithms over closed loop multiple-input multiple-output OFDM system [**13**]. In [**14**], the authors propose an unequal density of pilot placement for OFDM systems in time-varying channel to achieve UEP for important multimedia transmission. They also present a dynamic image data assignment scheme for UEP by utilizing visual saliency to relocate image data in an OFDM symbol for the UEP transmission. in [**15**] an unequal density of pilot placement for OFDM systems in time-varying channels and a dynamic image data assignment scheme is proposed to achieve UEP for important multimedia transmission. UEP for the Set Partitioning In Hierarchical Trees (SPIHT) bitstream is obtained in [**16**] by designing a multi-rate turbo coder which adopts multiple generators to enable it cover wide range of code-rates in an Alamouti STBC OFDM system. Salah *et al*. propose to combine convolutional coding with unequal cyclic time guard in an OFDM system to obtain UEP for image transmission [**17**]. In [**18**], a practical joint source-channel coding scheme for OFDM system is proposed and spatial diversity is exploited using space time block coding. [**19**] studies transmission of progressively coded image bitstreams using channel coding in a 2-D time-frequency resource block in an OFDM network. The authors in [**20**] use a single carrier frequency domain multiple access system to compare discrete fourier transform based systems with discrete cosine transform systems for an efficient image transmission. In [**21**], the authors propose to transmit wavelet based images using an adaptive OFDM system which allocates the modulation bit of each subcarrier according to the channel condition.

1.5. Space Time Block Coding for Transmit Diversity

Space Time Block Coding (STBC) is a technique used in wireless communication to transmit multiple copies of the transmitting data across multiple antennas at different time slots. This technique enhances the reliability of the wireless link, benefits the receiver through spatial diversity, and leads to a higher quality of the received signal. Implementation of the STBC technique occurs as the last step in the transmitter side of our proposed system. The space time block coding for two transmit antennas is defined as [**22**]:

$$\mathbf{C} = \begin{pmatrix} \boldsymbol{z}_1 & \boldsymbol{z}_2 \\ -\boldsymbol{z}_2^* & \boldsymbol{z}_1^* \end{pmatrix} \ , \tag{1-1}$$

where $\boldsymbol{z}_1$ and $\boldsymbol{z}_2$ are transmitted during the first time slot, from the first and the second antenna, respectively. Also $-\boldsymbol{z}_2^*$ and $\boldsymbol{z}_1^*$ are transmitted during the second time slot, from the first and the second antenna, respectively. $(.)^*$ also denotes complex conjugation.

The coded blocks of data are transmitted over the two channels during two consecutive time slots. The Channel Impulse Response (CIR) is assumed to remain constant during the two time slots. To keep the total transmit power constant in the multiple transmit antenna system, half of the power value used in the single antenna transmission scenario is provided to each transmitting antenna at each time slot. The received signal is thus formulated as follows:

$$\begin{aligned} \boldsymbol{r}_1 &= \boldsymbol{h}_1\boldsymbol{z}_1 + \boldsymbol{h}_2\boldsymbol{z}_2 + \boldsymbol{v}_1 \ , \\ \boldsymbol{r}_2 &= -\boldsymbol{h}_1\boldsymbol{z}_2^* + \boldsymbol{h}_2\boldsymbol{z}_1^* + \boldsymbol{v}_2 \ , \end{aligned} \tag{1-2}$$

where $\boldsymbol{r}_1$ is the received signal at the first time slot, and $\boldsymbol{r}_2$ is the received signal at the second time slot. $\boldsymbol{h}_1$ and $\boldsymbol{h}_2$ are the slow fading representation of the multi-tap channel; $\boldsymbol{v}_1$ and $\boldsymbol{v}_2$ indicate the Additive White Gaussian Noise (AWGN) of the channel at the first and the second time slot, respectively. At the receiver side, a linear combining is executed on the both received signals as follows [**22**]:

$$\begin{aligned} \hat{\boldsymbol{z}}_1 &= \boldsymbol{h}_1^*\boldsymbol{r}_1 + \boldsymbol{h}_2\boldsymbol{r}_2^* \ , \\ \hat{\boldsymbol{z}}_2 &= \boldsymbol{h}_2^*\boldsymbol{r}_1 - \boldsymbol{h}_1\boldsymbol{r}_2^* \ , \end{aligned} \tag{1-3}$$

where $\hat{\boldsymbol{z}}_1$ and $\hat{\boldsymbol{z}}_2$ are the recovered versions of $\boldsymbol{z}_1$ and $\boldsymbol{z}_2$. In the last step, the receiver recovers the information bits by a Minimum Mean Square Error (MMSE) or a maximum likelihood decoder.

1.6. List of Publications

1. M. Shayegannia, A. Hajshirmohammadi, S. Muhaidat, and M. Torki, "An OFDM Based System for Transmission of JPEG2000 Images Using Unequal Power Allocation," in *IEEE Wireless Communications and Networking Conference (WCNC)*, Paris, 2012, pp. 2064-2069.
2. M. Shayegannia, A. Hajshirmohammadi, and S. Muhaidat, "Using an Adaptive UPA Scheme with a Channel-Aware OFDM Technique for Wireless Transmission of JPEG2000 Images," presented at the *IEEE Canadian Conference on Electrical and Computer Engineering (CCECE)*, Montreal, 2012.
3. M. Shayegannia, S. Muhaidat, and A. Hajshirmohammadi, "Transmission of JPEG2000 Images in an Uplink Cellular Network with UPA and SCFDE: A System Description," presented at the *8th International Conference on Wireless and Mobile Communications (ICWMC)*, Venice, 2012.
4. M. Shayegannia, A. Hajshirmohammadi, S. Muhaidat, and M. Torki, "Transmission of JPEG2000 Images Over Frequency Selective Channels with Unequal Power Allocation," submitted to *IET Transactions on Image Processing*, 2012.
5. M. Shayegannia, S. Muhaidat, and A. Hajshirmohammadi, "Evaluation of OFDM and SCFDE on Transmission of JPEG2000 Images over Frequency Selective Channels," Under preperation, 2012.

2. Chapter 2: Transmission of JPEG2000 Images with UPA over Multi-Carrier Transmission Systems

Transmission of JPEG2000 images over frequency selective channels in a down-link cellular network from the base station to the mobile station has been widely investigated in the literature, as discussed in Section 1.4. Most of these works focus on protecting images during transmission using UEP technique, which lower the transmission data rate and leads to excessive usage of power for the coding bits. This chapter responds to the shortage of research on the UPA technique for wireless image transmission over frequency selective channels, by implementing a UPA technique in an OFDM system for different channel memory lengths and SNR values.

2.1. System Model

The overall system block diagram is presented in Figure 2-1, where the first stage is to transform the format of an input image into JPEG2000 format. Then, the Structural Information Retrieval unit removes the header information from data segment of the codestream and recovers the required information from the source coder, such as the number of code-blocks and the number of coding passes within each code-block. The header information is assumed to be received error free by the receiver. In the third stage, we apply the UPA optimization algorithm on the coded bitstream of the JPEG2000 image, where an optimal amount of power is allocated to each bit in order to minimize the total distortion of the received image. The output of the UPA optimization block is a vector containing the optimized power of all the bits of the codestream. This vector is then divided into several blocks using a serial to parallel buffer, and each block is diagonalized into a matrix, $\acute{\mathbf{E}}_n$, of size $N \times N$, where N is the number of subcarriers in

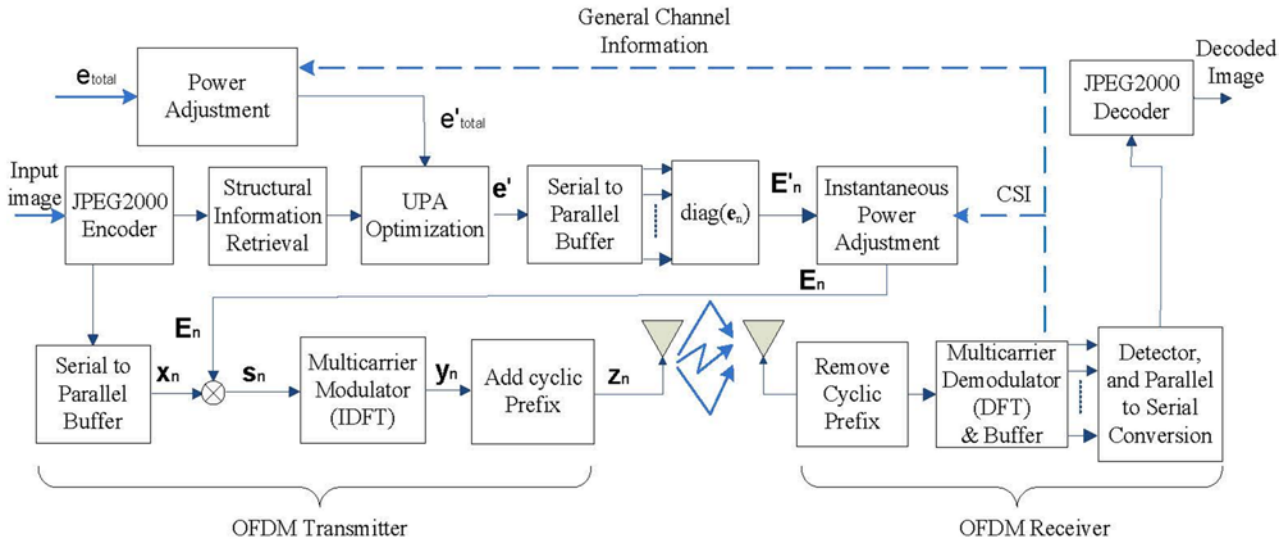

Figure 2-1: OFDM system block diagram

the OFDM transmitter. Once the instantaneous Channel State Information (CSI) from the n^{th} transmission block is received through a feedback channel, the Instantaneous Power Adjustment unit uses the instantaneous CSI to calculate the actual power of each bit in the n^{th} transmission block and produce the diagonal matrix $\mathbf{E}_n$. The feedback channel is assumed to be present in practice and have zero delay. In the OFDM transmitter, a serial to parallel buffer is used to divide the bitstream obtained from the JPEG2000 encoder into N_B parallel blocks, $\mathbf{x}_n = [x_1, x_2, \dots, x_N]^T$, where $n = 1, 2, \dots, N_B$. The power profile and data corresponding to each block are multiplied to form the vector $\boldsymbol{S}_n = \sqrt{\boldsymbol{E}_n}\mathbf{x}_n$, where $\mathbf{E}_n$ is an $N \times N$ diagonal matrix whose diagonal elements (defined later in (2-12)) are the actual power of the bits in the vector $\mathbf{x}_n$.

To modulate the N subcarriers by the bitstream, elements of $\boldsymbol{S}_n$ are transformed by Inverse Fast Fourier Transform (IFFT) to form $\boldsymbol{y}_n = \mathbf{Q}^H \boldsymbol{S}_n$, where $(.)^H$ denotes complex conjugate transpose operation. The adjacent subcarriers in $\boldsymbol{y}_n$ are apart exactly by one cycle. This property ensures the orthogonality between the subcarriers. The lower rate parallel subcarriers provide higher symbol duration which lessens the relative amount of dispersion in time caused by multipath delay spread. This, in addition to introducing a guard time in every OFDM symbol, eliminates ISI [**23**]. A cyclic prefix is appended to the beginning of each OFDM sample (to the elements of $\boldsymbol{y}_n$), to form the

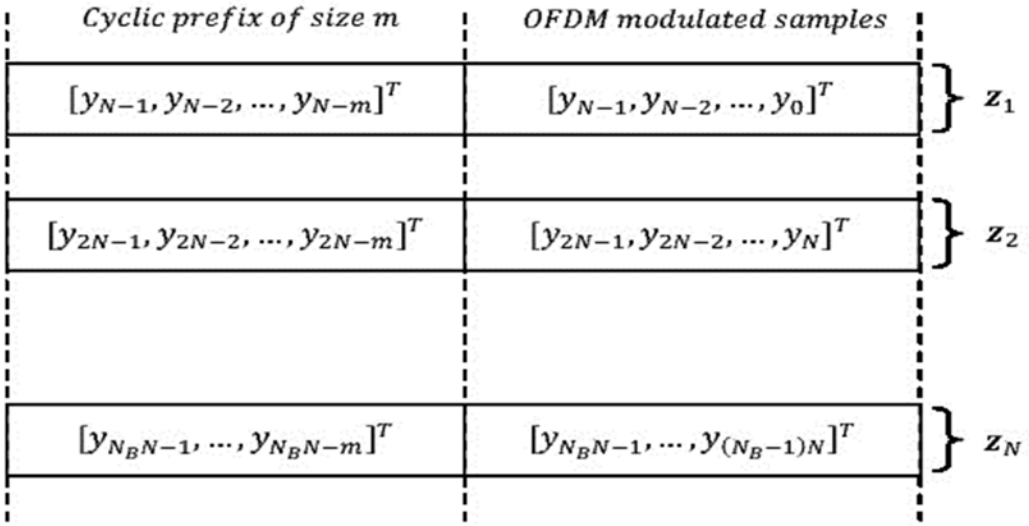

Figure 2-2: Transmission block format of OFDM symbols

transmitting sequence, $\boldsymbol{z}_n$, with a size of $N+m$, as illustrated in Figure 2-2. The cyclic prefix consists of the last m symbols of every OFDM sample ($m < N$). The size of

the cyclic prefix , m, is equal to the memory of the channel or the number of taps in the multipath channel.

We assume the wireless communication channel to be frequency selective fading, and equip all terminals with single transmit and receive antennas. The CIR for the n^{th} transmission block is given by $\boldsymbol{h}_n = [h_0,\ h_1,\ h_2, \dots,\ h_{m-1}]^T$ where m is the channel memory length and $n = 1, 2, \dots, N_B$. The entries of the random vectors $\boldsymbol{h}_n$ are assumed to be independent zero-mean complex Gaussian random variables and remain constant over a single data block, and vary independently for every block. The received signal at the destination terminal is given by:

$$\boldsymbol{r}_n = \mathbf{H}_n \mathbf{Q}^H \sqrt{\boldsymbol{E}_n}\mathbf{x}_n + \mathbf{v}_n \ , \tag{2-1}$$

where $\boldsymbol{r}_n$ is the n^{th} received block of data, $\mathbf{H}_n$ is an $N \times N$ circulant matrix for the n^{th} transmission block with entries $[\mathbf{H}_n]_{ik} = [\boldsymbol{h}_n]_{(i-k)\ mod\ N}$ and $[\boldsymbol{h}_n]_i = 0$ for $i > m-1$. $\mathbf{v}_n$ is an $N \times 1$ Additive White Gaussian Noise (AWGN) vector with mean of zero and variance of 1/2 per dimension. The channel structure in (2-1) is formed as a circulant matrix, which accounts for the addition of the cyclic prefixes to the OFDM symbols ($\boldsymbol{y}_n$).

The OFDM receiver transforms the received samples to the frequency domain by applying the Fast Fourier Transform (FFT), i.e, multiplying by the $\mathbf{Q}$ matrix.

$$\mathbf{Q}\boldsymbol{r}_n = \Lambda_n\sqrt{\boldsymbol{E}_n}\mathbf{x}_n + \mathbf{Q}\mathbf{v}_n \ , \tag{2-2}$$

where $\Lambda_n = \mathbf{Q}\mathbf{H}_n\mathbf{Q}^H$ is a diagonal matrix of size $N \times N$ for the n^{th} transmission block, in which the diagonal elements are [**24**]:

$$[\Lambda_n]_{ii} = \sqrt{N}\mathbf{q}_i^H\left(\mathbf{h}_n \overbrace{0\ 0\ \dots\ 0}^{N-m}\right)^{\boldsymbol{T}}, \qquad i = 1, 2, \dots, N \tag{2-3}$$

where $\mathbf{q}_i$ is the i^{th} column of the matrix $\mathbf{Q}$. Due to the different realizations of the CIRs for each block of data, the diagonal elements of Λ change for every block n of the received signal, and they can be considered as the gains of an equivalent slow flat fading channel. Moreover, these elements are in fact the eigenvalues of the channel matrix $\mathbf{H}$. Overall, note that OFDM converts the underlying frequency selective channels into parallel flat fading channels [**24**].

At the receiver side, once the coefficient realizations of the slow fading paths are identified, the OFDM receiver feeds back the instantaneous CSI to the Instantaneous Power Adjustment unit. Note that data can be recovered using a simple zero forcing equalizer and can be sent to the JPEG2000 decoder to produce the output image. One of the advantages of our proposed system is that the recovered data does not need a dedicated source decoder and can be decoded by any standard JPEG2000 decoder.

2.2. Distortion Model

This section presents a distortion model for calculating the total distortion of the JPEG2000 decoded bitstream based on the power assigned to bits of each coding pass. The distortion model is given by:

$$E\{D_{total}\} = d_0 + \sum_{i=1}^{R}\sum_{j=1}^{R_i} p_{ij}D_{ij}\prod_{k=1}^{j-1}(1 - p_{ik}) \ , \tag{2-4}$$

where $E\{D_{total}\}$ is the expected value of the total distortion of the decoded image, d_0 is an unavoidable distortion due to quantization during source coding, R is the total number of Code-Blocks (CB) in the bitstream, and R_i is the number of Coding Passes (CP) in the i^{th} code-block, CB_i. p_{ij} is the probability that there is at least one bit error in CP_{ij}, the j^{th} coding pass in the i^{th} code-block. D_{ij} is the distortion due to any bit error in CP_{ij}.

The Structural Information Retrieval block, included within the system block diagram in Figure 2-1, retrieves the values of R and R_i from the JPEG2000 encoder and supplies them to the UPA unit to compute the distortion. To calculate d_0, we measure the Mean Square Error (MSE) between the original image (distortion-free) and its decoded version without any channel fading and AWGN effect. In order to calculate the distortion corresponding to each coding pass, D_{ij}, we manually alter at least one bit in that coding pass, and keep the rest of the image bitstream error free. Then, the distortion due to that coding pass is determined by measuring the MSE between the decoded image and the original image. Note that as long as there is at least one bit error in a particular coding pass, the distortion due to that coding pass is the same regardless of the numbers and positions of the bit errors within the coding pass. As a result, our algorithm allocates similar power to all bits within the same coding pass, which results into a similar probability of error for all bits within the same coding pass. The expression for p_{ij} can be given as:

$$p_{ij} = 1 - \left(1 - p_{eb}(i,j)\right)^{N_b(i,j)} \quad , \tag{2-5}$$

where $p_{eb}(i,j)$ and $N_b(i,j)$ are the Bit Error Rate (BER) and the number of bits in CP_{ij}, respectively. Since the optimization problem is formulated under the assumption of AWGN channel, $p_{eb}(i,j)$ should represent the BER for an AWGN channel which is

$$p_{eb}(i,j) = Q\left(\sqrt{\frac{2\acute{e}_{ij}}{N_0}}\right) \quad , \tag{2-6}$$

where N_0 is the noise power, $\acute{e}_{ij}$ is the assigned power for bits within CP_{ij}, and $Q(x)$ is the Q-function which represents the probability that a standard Normal random variable will obtain a value larger than x.

2.3. Unequal Power Allocation Implementation

This section elaborates on the UPA optimization algorithm which was proposed in [**25**]. We demonstrate the effectiveness of this algorithm in minimizing the total end to end distortion in (2-4), and then improve the algorithm by proposing an adaptive UPA. In addition, a time complexity analysis of the algorithm is provided in this section.

2.3.1. Unequal Power Allocation Optimization Algorithm

As previously explained, the objective here is to minimize the expected value of the total distortion of the decoded bitstream by assigning optimal amount of power to each coding pass. Equation (2-7) formulates our objective into an optimization form as follows:

$$\underset{\acute{e}_{ij}}{\text{minimize}}\, E\{D_{total}\}$$
$$\text{subject to} \begin{cases} \acute{e}_{total} = \sum_{i=1}^{R} \sum_{j=1}^{R_i} \acute{e}_{ij} N_b(i,j) \\ \acute{e}_{ij} \geq 0, i = 1, \dots, R \;\; j = 1, \dots, R_i \end{cases}, \tag{2-7}$$

where $E\{D_{total}\}$ was introduced in (2-4) and $\acute{e}_{total}$ is the adjusted total available power to the UPA unit, and it is defined later in (2-10). In order to solve (2-7), Torki proposes to use Simulated Annealing (SA) method ([**26**]), which is a generalization of Monte Carlo method and is used to locate a good approximation of the global minimum of an object function in a large search space [**25**]. Because there is a large number of coding passes in a JPEG2000 coded image (e.g, 250 coding passes in Lena ($512 \times 512, 0.25$ bpp), and each coding pass has a different number of bits, calculating the optimal value of power for every single coding pass is computationally extensive. In order to reduce the computational complexity, coding passes are categorized into L number of groups, and the SA optimization algorithm attempts to find the optimal power values for each group. To choose a reasonable value for L, its value should be small enough to keep the complexity low while not jeopardizing the accuracy of the algorithm. Thus, the algorithm was tested for transmission of Lena ($512 \times 512, 0.25$ bpp) for different number of groups (L) at different SNR values. It was determined that the performance improves as the number of

groups increases; however, when the number of groups exceeds 10, the improvement in the performance becomes negligible [**25**]. As a result the number of groups, L, was proposed to be 10 in [**25**], and the same value is used here. The SA algorithm can be summarized as follows:

Table 2-1: Simulated Annealing UPA Algorithm

$\acute{e}_{current} = \acute{e}_{initial}$
$D_{current} = D(\acute{e}_{current})$
$D_{min} = D(\acute{e}_{initial})$
$D_{old} = 10^{10}$
$Iter = 0$
While $(iter \leq iter_{max})$ **do**
    $\acute{e}_{new} =$ choose Random Neighbor $(\acute{e}_{current})$
    $\acute{e}_{norm} =$ normalize $(\acute{e}_{new})$
    $D_{min} = D(\acute{e}_{initial})$
    if $(D_{new} < D_{min})$ **then**
        $\acute{e}_{best} = \acute{e}_{norm}$
        $D_{min} = D_{new}$
    end if
    if $(D_{new} < D_{current})$ **or** (with certain probability)
        $\acute{e}_{current} = \acute{e}_{norm}$
        $D_{current} = D_{new}$
    end if
    $iter++$
    if $\left(\text{remainder}\left(\frac{iter}{20}\right) = 0\right)$
        if$(|D_{new} - D_{old}| < 0.1)$
            $iter = iter_{max} + 1$
        end if
        $D_{old} = D_{new}$
    end if
end while

In the above algorithm, $\acute{e}_{initial}$ is a column vector of size L which includes initial power values assumed for bits within each group. A function is then employed which assigns random neighboring values to the vector $\acute{e}_{initial}$ and generates $\acute{e}_{new}$. Then, the algorithm checks whether the distortion resulting from the new power values could potentially be the minimum distortion. At the end of the iterations, the set of power values which resulted in the minimum distortion is assigned as the final power for each group.

The function by which $\acute{e}_{new}$ is obtained from its random neighboring values can be formulated as [**25**]:

$$\acute{e}_{new} = \acute{e}_{current} + \left(\varepsilon - \frac{iter}{iter_{max}}\right)\frac{\acute{e}_{total}}{L}\mathbf{z}, \tag{2-8}$$

where L is the number of groups, and $\mathbf{z} = [z_1,\ z_2, \dots, z_L]^{\mathrm{T}}$ is a random vector which is uniformly distributed between $(-\beta, +\beta)$. The algorithm is not sensitive to the constant parameters ε and β, and in our experiments we set $\varepsilon = 1.5$, and $\beta = 0.1$ [**25**].

The form of the function in (2-8) suggests that the SA optimization algorithm, initially, starts with a large search space and chooses the neighboring values from a wide random range. As the number of iterations increases, the search space becomes narrower. The uncertainty with a specific probability (set to be 0.05) is added to the second "if" statement of the algorithm to let the algorithm escape from local minima. Furthermore, the line, $\acute{e}_{norm} = \mathrm{normalize}\,(\acute{e}_{new})$, is added to ensure that summation of power values will add up to the total available power in every iteration. The normalization is performed as follows:

$$[\acute{e}_{norm}]_i = \frac{[\acute{e}_{new}]_i \times \acute{e}_{total}}{\sum_{i=1}^{L}[\acute{e}_{new}]_i}, \tag{2-9}$$

The UPA optimization algorithm is implemented in real time and needs to be executed only once for multiple transmissions of every image over wireless channels. This enlightens one of the advantages of this algorithm in the case of multiple users at the receiver side.

We illustrate the process undertaken by the UPA optimization algorithm in Table 1, Figure 2-3, and Figure 2-4. Note that the algorithm avoids getting stuck in local mini-

ma and searches for the right amount of power for each group resulting in a lower total distortion. Also, at lower values of SNR, the algorithm requires a larger number of iterations to find the minimum distortion compared to the higher SNR values. For example, for the image of Lena at SNR = 16 dB, the algorithm takes only 100 iterations to find the minimum distortion, whereas at SNR = 9 dB, the iterations increases up to 340. The latter iteration value changes to 237 for the image of Peppers. As a result, at higher transmission power values, the computational load of the UPA algorithm reduces. The reason that higher SNR values lead to lower iteration values is that the initial total end to end distortion in (2-4) is calculated at a lower value at higher SNR values. Thus it takes the algorithm less number of iterations to find the minimum value for the distortion, compared to the case where lower SNR values are utilized.

2.3.2. Time Complexity Analysis

We examine the time complexity of the UPA algorithm for transmission of images of Lena and Peppers ($512 \times 512, 0.25$ bpp) by averaging the amount of time consumed to run the algorithm over 1000 iterations. For this purpose, we employ a personal computer that runs Microsoft© Windows© 7 with an Intel© Core i7 quad-core 740QM/1.73 GHz CPU, 4 GB RAM size, that runs Matlab© 2010a.

The investigations indicate that the time consumption of the algorithm is independent of the input image to the system, and the amount of power available to distribute over the coding passes. For example, the UPA algorithm consumes 0.2078 seconds to operate at an SNR value of 20 dB and $L = 10$ for the image of Lena. Decreasing the value of L to 2 or increasing it to 60 changes the consumption time of the algorithm by ∓ 0.02 seconds. Our analyses indicate that variation on the value of power by ± 50 dB causes a slight variation on the time consumption by ∓ 0.01 second. For the image of Peppers, the algorithm consumes 0.2194 seconds to run with $L = 10$ at an SNR value of 20 dB. Altering the number of groups between 2 and 60 or changing the amount of available power for Peppers by ± 50 dB changes the time by ∓ 0.005 or ∓ 0.01 second, respectively.

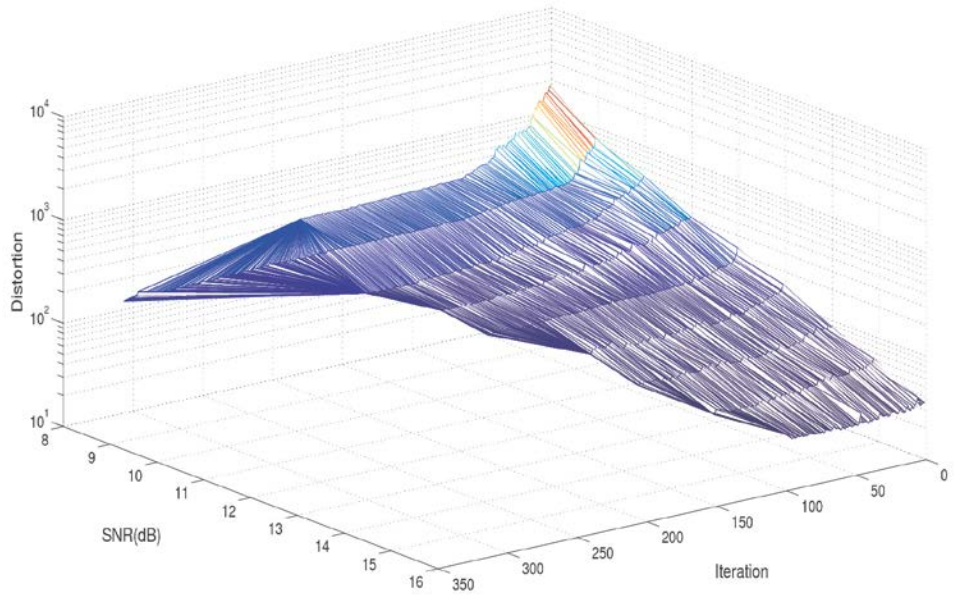

Figure 2-3: Using Algorithm 1 on Lena $(512 \times 512, 0.25\ bpp)$ ***to minimize distortion for SNR values between 8 and 16 dB, during different iterations***

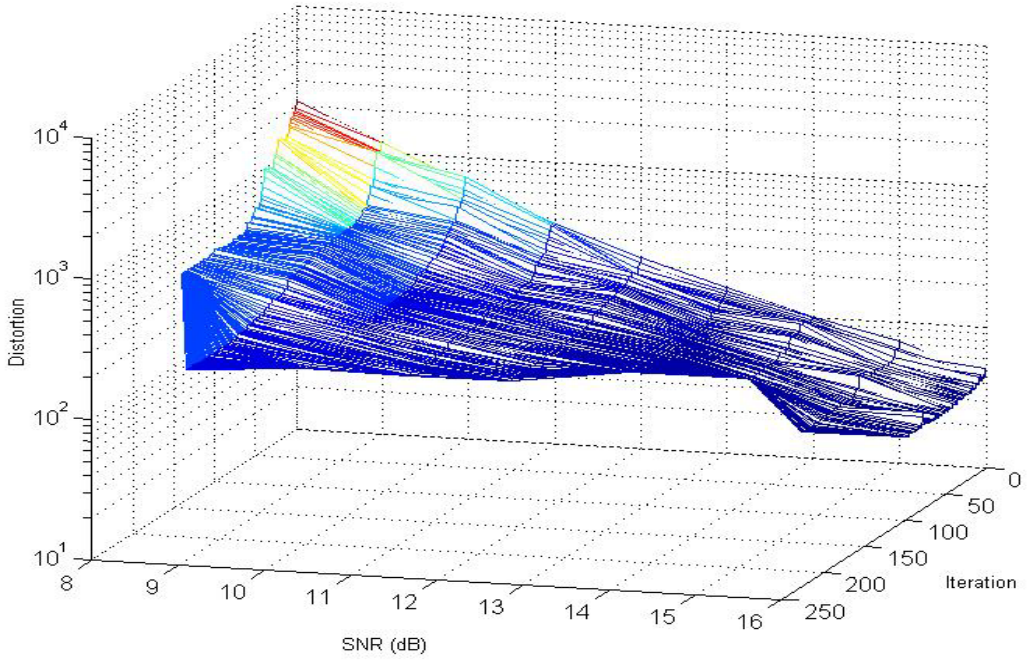

Figure 2-4: Using Algorithm 1 on Peppers $(512 \times 512, 0.25\ bpp)$ ***to minimize distortion for SNR values between 8 and 16 dB, during different iterations***

2.3.3. Adaptive Unequal Power Allocation

To lower the computational load of the optimization algorithm, the coding passes were categorized into $L = 10$ number of groups in the previous section. In this section, we incorporate an adaptive scheme into the UPA algorithm such that for every SNR value a different group number that contributes to a higher PSNR of the received image is chosen. For this purpose, we analyze the UPA algorithm performance by transmitting 1000 images of the Lena and Peppers at $512 \times 512, 0.25$ bpp, image of the Bridge at $176 \times 144, 0.25$ bpp, and image of the Couple $176 \times 144, 0.15$ bpp through block fading non-frequency selective channels and average the resulting PSNR values.

Figure 2-5, Figure 2-6, Figure 2-7, and Figure 2-8 present variations of PSNR of the received Lena, Peppers, Bridge, and Couple respectively, for every group number at SNR values between 8 dB and 20 dB. Our analyses of time complexity for the UPA algorithm indicate that the time consumption of the algorithm for different number of groups between 2 to 100 varies only between ∓ 0.02 seconds. However, the higher group numbers impose more computational load on the algorithm. Thus, in this adaptive scheme, the number of groups is limited to vary between 2 and 30 to bound the computational load of the algorithm. The circle points indicate the desired value of L for a particular SNR at which maximum quality of the received image is achieved. Figure 2-5 to Figure 2-8 indicate that values of L less than 4 result into an increased distortion of the received image at low range SNR values, and at SNR values higher than 14 dB, a smaller enhancement in the PSNR profile is achieved as the number of groups increases.

The results suggested by Figure 2-5, Figure 2-6, Figure 2-7, and Figure 2-8 are reformed into Figure 2-9, Figure 2-10, Figure 2-11, and Figure 2-12 respectively, in order to obtain a direct relationship between the available SNR value and its advantageous group number. Note that values of L at different SNR values are subjective to the transmitting image. Our investigations reveal that about 100 iterations is sufficient to obtain a close to accurate value for L at each SNR. Reducing the number of iterations makes the adaptive scheme practical to run an offline training stage for every image before the transmission, in order to generate the relationship between L and SNR. Then to transmit a particular image, the UPA algorithm refers to the decided values for the group numbers at different SNR values of the channel.

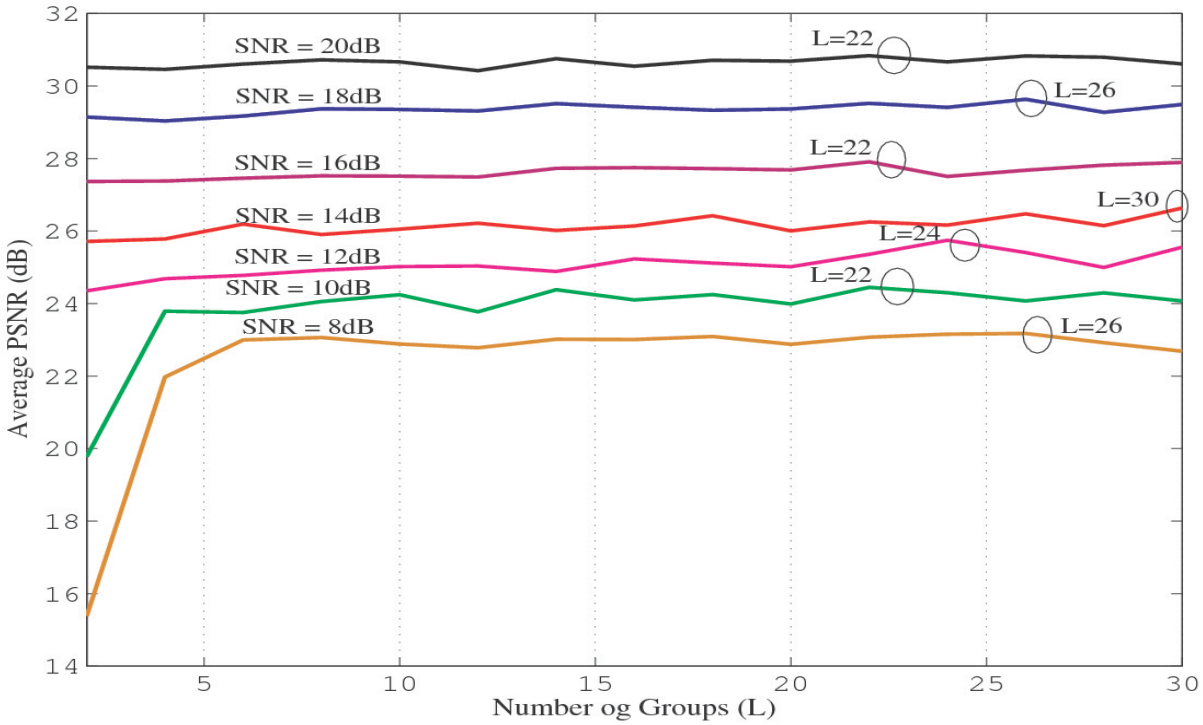

Figure 2-5: Evaluation of PSNR value of the received "Lena" ($512 \times 512, 0.25$bpp) at different group numbers

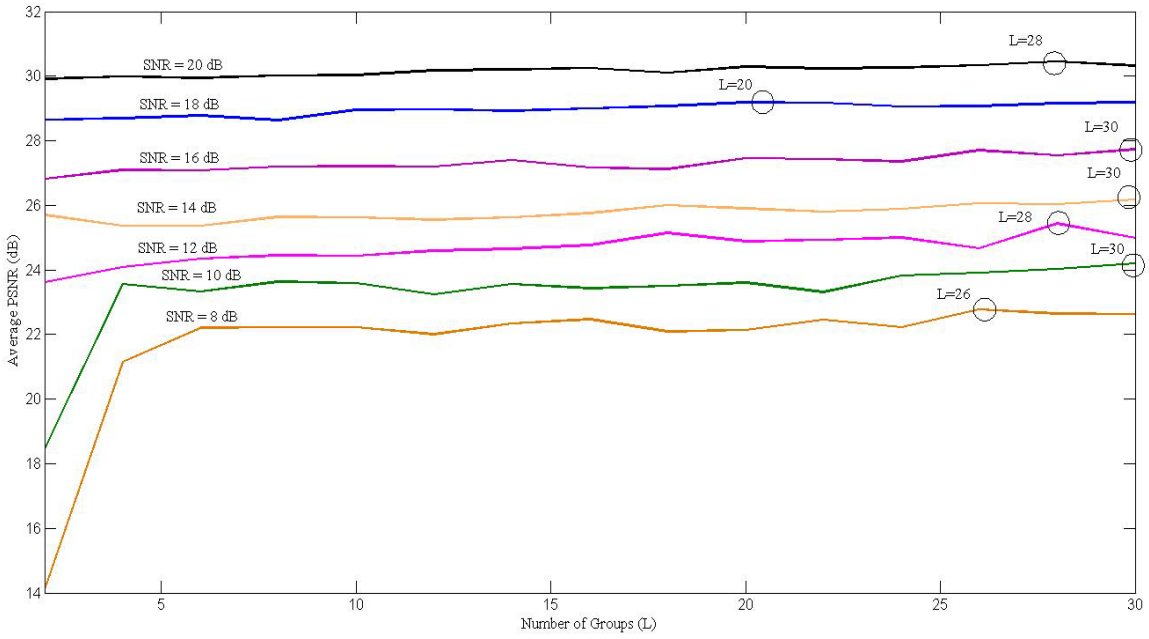

Figure 2-6: : Evaluation of PSNR value of the received "Peppers" ($512 \times 512, 0.25$ bpp) at different group numbers

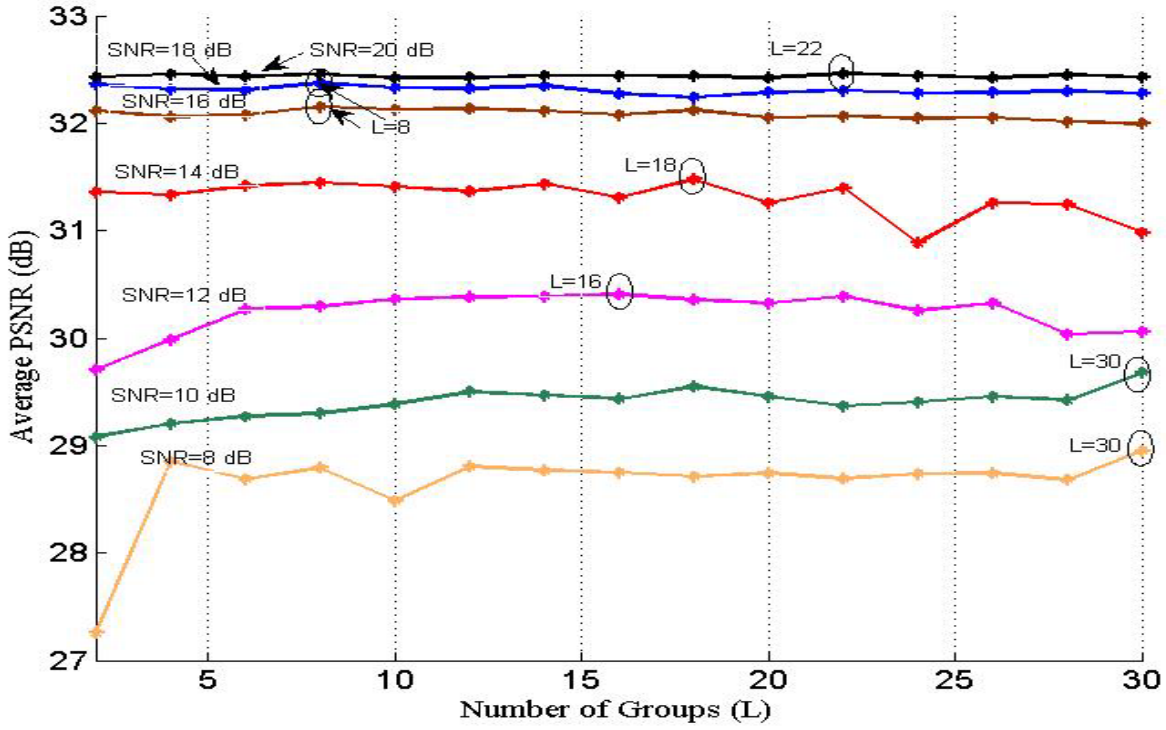

Figure 2-7: Evaluation of PSNR value of the received "Bridge" ($176 \times 144, 0.25$ bpp) at different group numbers

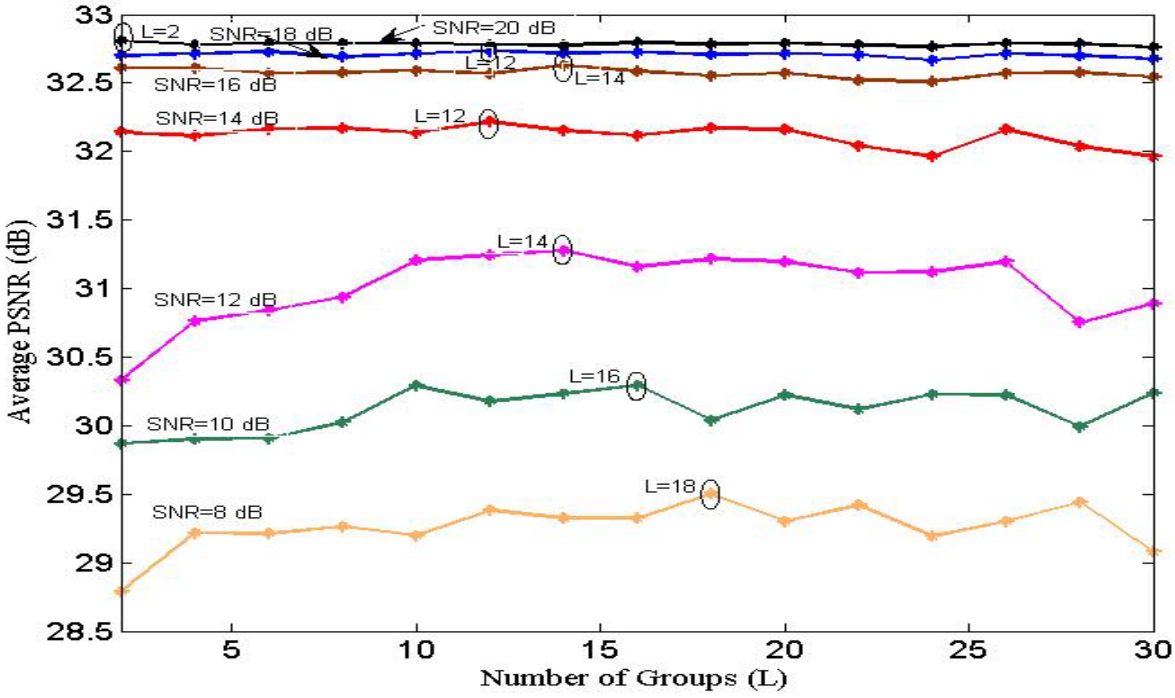

Figure 2-8: Evaluation of PSNR value of the received "Couple" ($176 \times 144, 0.15$ bpp) at different group numbers

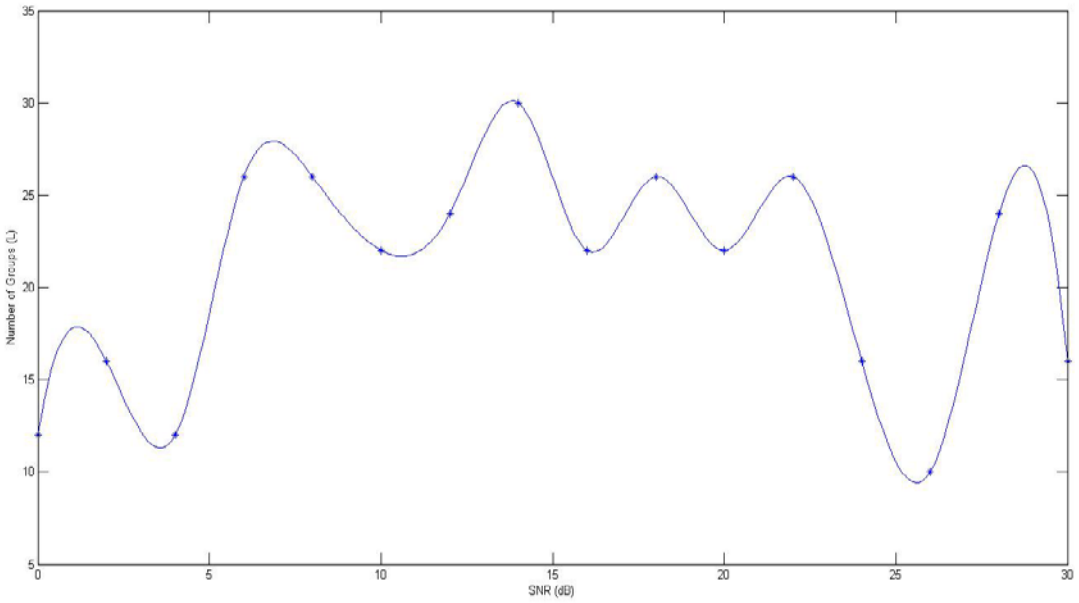

Figure 2-9: The appropriate number of groups resulting in the maximum PSNR at each SNR value of the received "Lena" ($512 \times 512, 0.25$ ***bpp)***

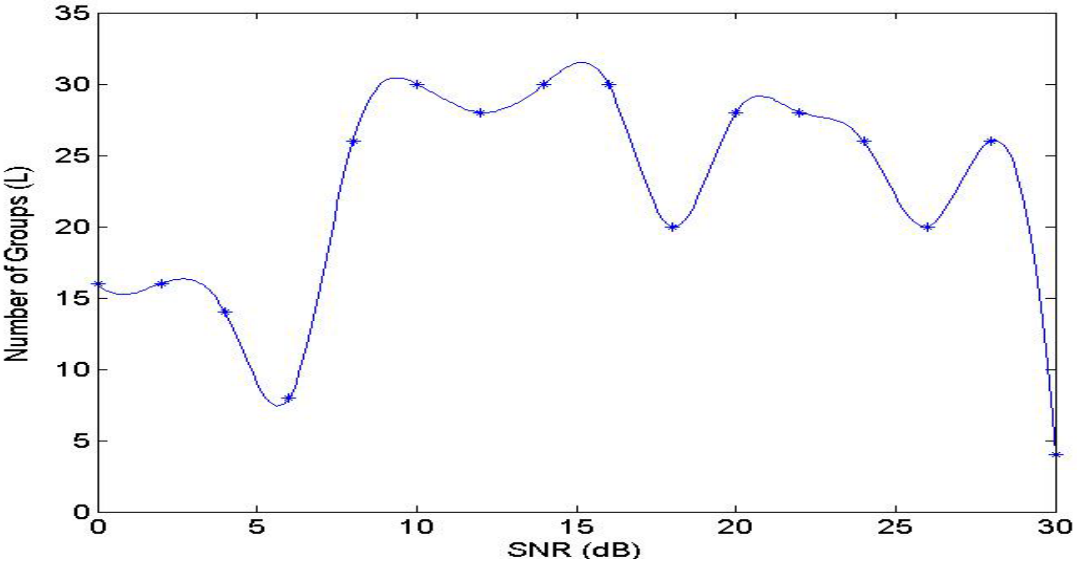

Figure 2-10: The appropriate number of groups resulting in the maximum PSNR at each SNR value of the received "Peppers" ($512 \times 512, 0.25$ ***bpp)***

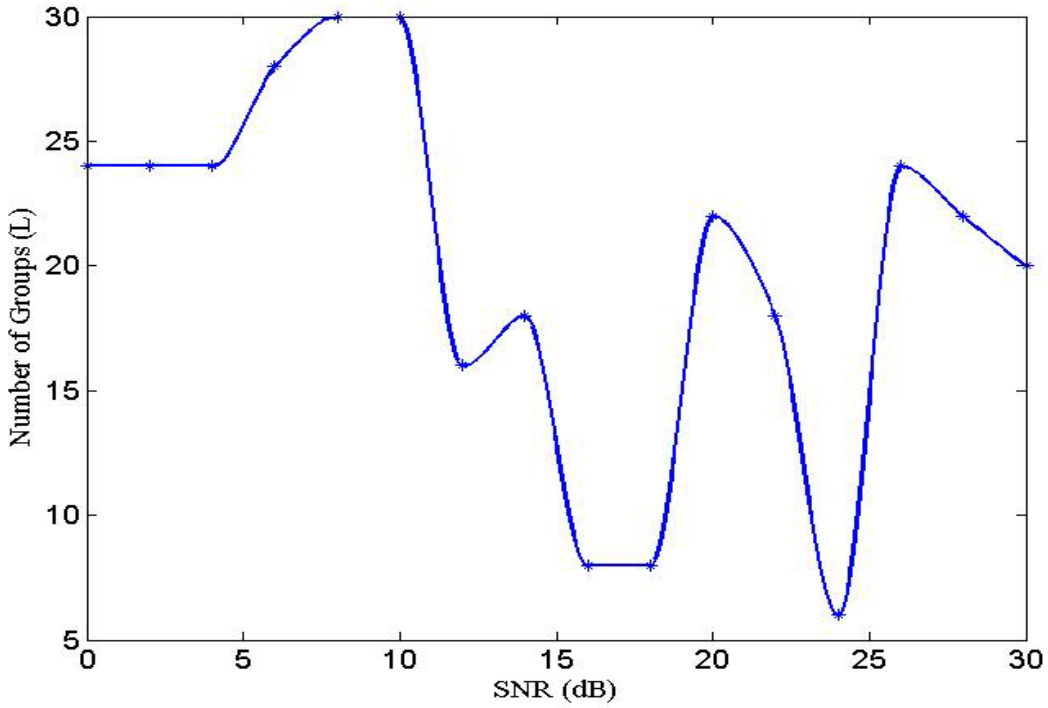

Figure 2-11: The appropriate number of groups resulting in the maximum PSNR at each SNR value of the received "Bridge" ($176 \times 144, 0.25$ ***bpp)***

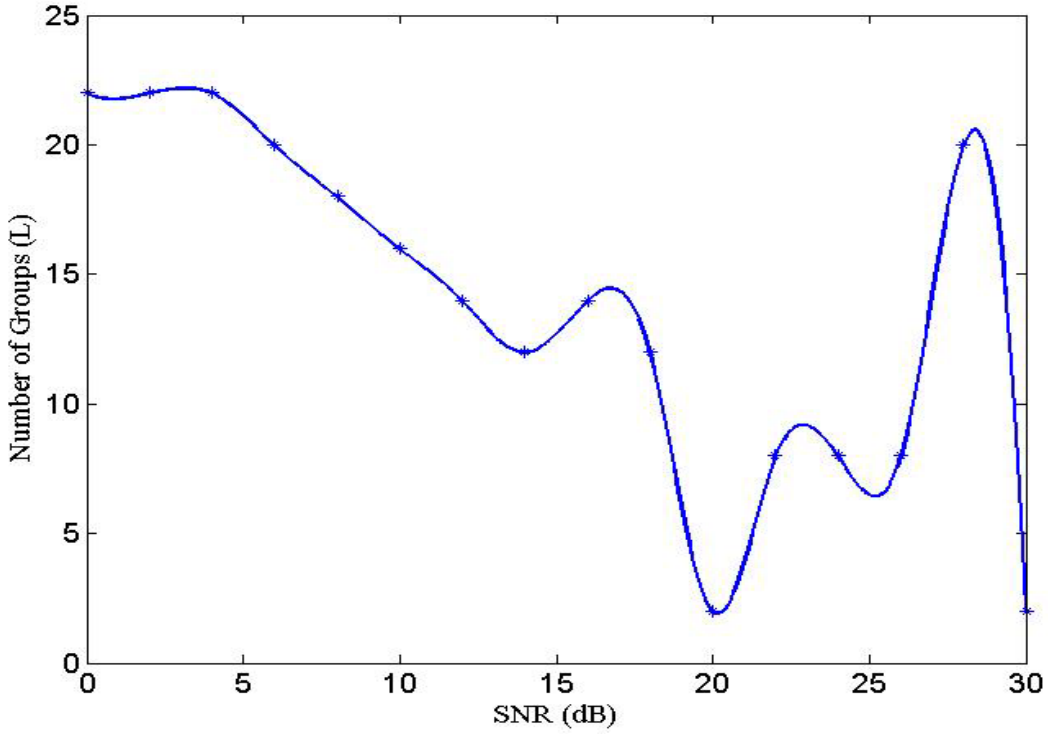

Figure 2-12: The appropriate number of groups resulting in the maximum PSNR at each SNR value of the received "Couple" ($176 \times 144, 0.15$ ***bpp)***

To find out the advantage of the proposed adaptive scheme over our UPA algorithm, 1000 images of Lena, Peppers, Bridge, and Couple at different sizes and source coding rates are transmitted over block fading non-frequency selective channels. The average PSNR values of the received images using the adaptive and the non-adaptive UPA scheme are presented in Figure 2-13. This figure indicates that the adaptive scheme yields a substantial enhancement in the PSNR performance at lower range SNR values. As the power available to transmit an image increases (higher SNR values), the improvement introduced by our adaptive scheme on the PSNR performance becomes insignificant. For example, the adaptive scheme improves the PSNR performance of the received Lena and Peppers for 2.5 dB at an SNR value of 2 dB. As the SNR increases to 12 dB and 20 dB, the PSNR improves only by 0.7 dB and 0.15 dB, respectively. However, these performance improvements are not as significant for the images of the Bridge and the Couple.

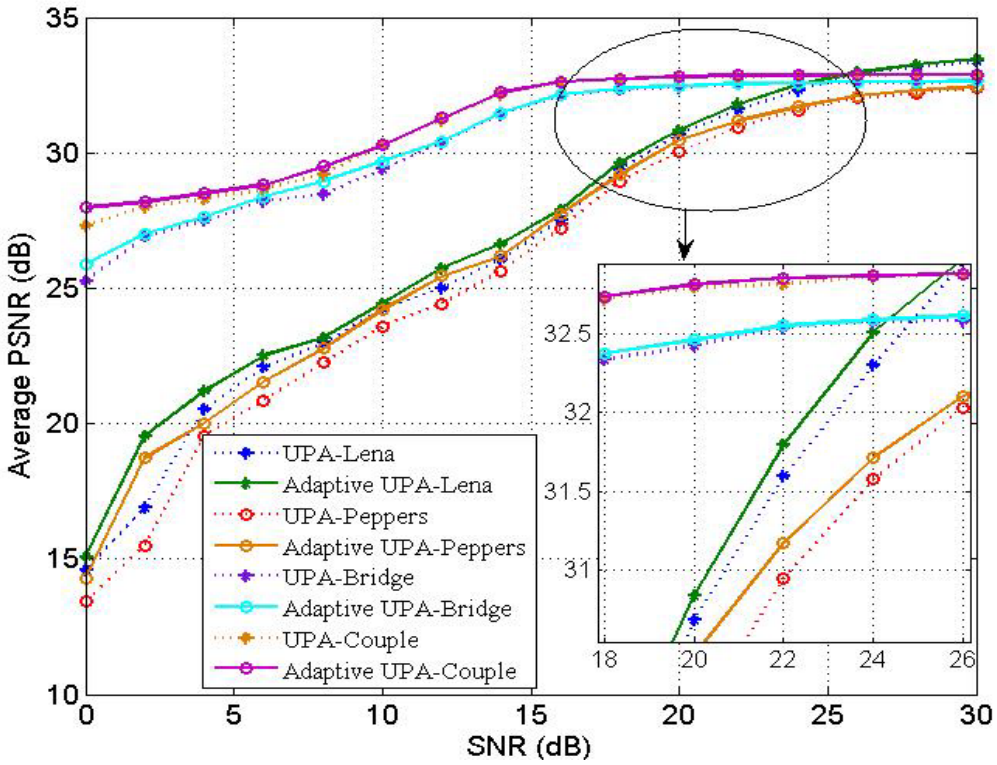

Figure 2-13: Evaluation of PSNR value of the received "Lena" and "Peppers" ($512 \times 512, 0.25$ bpp), with UPA and adaptive UPA algorithms

2.4. Power Adjustment Unit

Before implementing the UPA algorithm, the Power Adjustment unit, in ure 2-1, uses the statistical information of the channel to adjust the total power available for transmission of the image (e_{total}), to the total power available to the UPA unit ($\acute{e}_{total}$). This adjustment is performed to account for the average fading effect of the channel.

$$\acute{e}_{total} = e_{total}\left(E\left\{\frac{1}{h^2+\alpha}\right\}\right)^{-1}, \tag{2-10}$$

where

$$E\left\{\frac{1}{h^2+\alpha}\right\} = \int_{0^+}^{\infty} \frac{1}{h^2+\alpha}\frac{h}{\sigma^2}e^{-\frac{h^2}{2\sigma^2}}dh = e^{\alpha}\int_{\alpha}^{\infty}\frac{e^{-h}}{h}dh\,. \tag{2-11}$$

In (2-10) and (2-11), h is a random variable with Rayleigh distribution, and it represents the channel's fading factor. σ is the parameter of the Rayleigh distribution model which is equal to $\sqrt{0.5}$ for unity variance channel coefficients. α is a small constant added to avoid near zero values in the denominator when the fading factor is very small, as a result, avoiding very large adjusted power. From a practical point of view, a very large adjusted power will cause the power amplifier to operate outside its linear region and bestow a degraded performance. To choose a value for α, the results of the optimization algorithm is evaluated for different values of α in [**9**]. It was determined that the algorithm is not highly sensitive to value of the constant parameter α, and its value was set to 0.01, small enough to be insignificant against the fading coefficients.

2.5. Instantaneous Power Adjustment

As indicated before, the optimization problem in (2-7) is formulated under the assumption of AWGN channel with no fading. The effect of fading, however, should be taken into account at the time of transmission. This effect is manifested on both e_{total} and $\mathbf{\acute{E}}_n$. Section 2.4 discusses how the Power Adjustment unit modifies the total amount of available power in order to take into account the effect of the average fading. After the algorithm assigns unequal powers to bits within each coding pass, a serial to parallel

buffer divides the vector $\boldsymbol{\acute{e}}_{ij}$ into N_B blocks, each of size $N \times 1$. The n^{th} block is then diagonalized into the matrix $\mathbf{\acute{E}}_n$, once the CSI for the corresponding block is received.

Instantaneous Power Adjustment unit compensates for fading by using instantaneous values of the fading factor from the m-tap channels. The compensation is performed in (2-12) by dividing the assigned power of each bit by the magnitude of the channel coefficient corresponding to the time interval in which the bit is transmitted. This division will increase or decrease the assigned power to each bit depending on whether the fading factor is larger or smaller than unity, respectively. Since, a block fading wireless channel is considered for the transmission medium, we assume that the fading coefficients remain constant during every time interval (T). This time interval incorporates training sequence for channel estimation, feedback delay, and transmission of data. As a result, once the negative effect of fading is compensated, the algorithm performs as good as if the transmission channel is AWGN.

$$[\mathbf{E}_n]_{ii} = \frac{\left[\mathbf{\acute{E}}_n\right]_{ii}}{|[\Lambda_n]_{ii}|^2 + \alpha} \qquad i = 1, 2, \dots, N. \tag{2-12}$$

In (2-12), $[\Lambda_n]_{ii}$ is the fading factor defined in (2-3), $\left[\mathbf{\acute{E}}_n\right]_{ii}$ is the assigned power to the i^{th} bit from the n^{th} transmission block, and $[\mathbf{E}_n]_{ii}$ represents the corresponding power of each bit after the effect of fading is taken into account. We call $[\mathbf{E}_n]_{ii}$ the *actual* power of i^{th} bit from the n^{th} transmission block.

Note that the UPA unit is assuming the CSI is available to the receiver and can be fed back to the transmitter. Since the channel impulse response of the n^{th} transmission block, $\mathbf{h}_n$, is assumed to be constant over a block of data, CSI is to be fed back to the transmitter once for every transmitting block. That is, having N symbols in every block, the receiver has to feedback N coefficients of the channel fading factors to the transmitter at every time interval before the transmission instant. There are many papers in the literature on estimate CSI using pilot assisted techniques or blind estimation methods (e.g, [**27**], [**28**]).

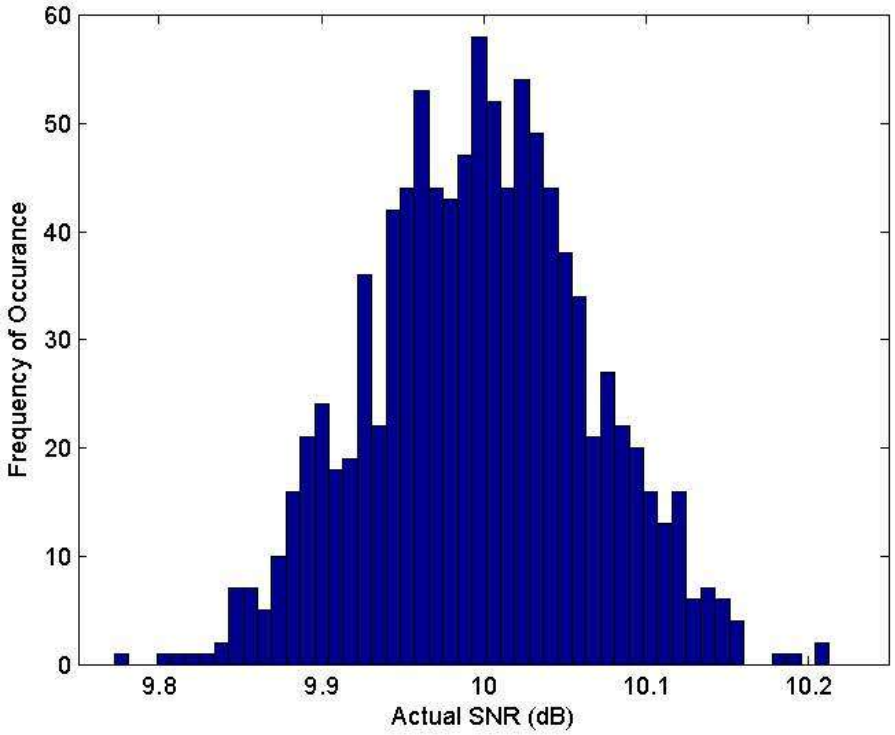

Figure 2-14: Actual power consumed for the transmissions of Lena $(\mathbf{512 \times 512, 0.25}\ \boldsymbol{bpp})$ ***at an average SNR of*** $\mathbf{10}$ ***dB***

In order for the original power constraint to be preserved, the summation of the actual powers assigned at the time of transmission must be equal to e_{total}. To verify this, Figure 2-14 presents a histogram of the actual total power consumed (i.e, $\sum_{n=1}^{N_B}\sum_{i=1}^{N}[\mathbf{E}_n]_{ii}$) at each transmission of Lena, sent 1000 times assuming available SNR=10 dB, which translates to $e_{total} = 10\log(60224 \times 10) = 5.80$ dB, where 60224 is the total number of bits per coded bitstream of the Lena ($512 \times 512, 0.25$ bpp).

The histogram in Figure 2-14 has a mean of 9.9981 dB which is very close to the original SNR value assumed for each bit, and a coefficient of variation of 0.0156. Coefficient of variation is a normalized measure of dispersion of a distribution, and it is defined as the ratio of the standard deviation to the mean. As a result, the actual consumed power at the time of transmission is on average very close to the total available power, e_{total}.

Table 2-2: Comparison of the average power consumed by each bit with their corresponding primary power values

SNR based on original e_{total} (dB)	Average SNR based on actual consumed power (dB)	Coefficient of Variation
0	0.00046	0.0029
10	9.9981	0.0156
20	20.0013	0.00095
30	30.0007	0.0010

Table 2-2 also shows that the mean value of the average power consumed by each bit for transmission of Lena is very close to the corresponding original power values.

2.6. Channel Aware Transmission

This section discusses our proposed channel assignment strategy within the OFDM transmitter. Advantage of an OFDM system lies on its ability to transform a wideband frequency selective channel into multiple narrow band slow fading channels. For this purpose, the available wide band channel bandwidth (W) is divided into narrow band subbands of $\Delta f = \frac{W}{N}$, where N is the number of narrow band subbands. With each subband, we associate a sinusoidal carrier signal (subcarrier) of the form [**23**]:

$$\mathbf{c}_i(t) = cos 2\pi f_i t \qquad i = 0, 1, \dots, N-1, \tag{2-13}$$

where f_i is the mid frequency in the i^{th} subchannel. Having the adjacent subcarriers apart exactly by one cycle ensures the orthogonality between the subcarriers. Parallel subcarriers are modulated by the bitstream and transformed by the IFFT matrix. Each subcarrier experiences a relatively flat fading subchannel. By measuring the SNR of each subchannel at the receiver, and communicating this information with the transmitter, the transmitter can perform a channel assignment strategy to optimize the transmission process. This strategy detects the more important symbols in every transmission

block of data and passes them over the subcarriers with higher channel gain. The channel assignment strategy can be summarized as follows

Table 2-3: Channel Assignment Strategy at the Transmitter

$n = 1$
for (every block n of transmitting data symbol , $n = 1, 2, \dots, N_B$) **do**
In the receiver:
1- Measure SNR of each subchannel
2- Communicate the CSI through a feedback channel with the transmitter
In the transmitt:
1- Sort the subcarrier channel gains from the largest coefficient to the smallest
2- Sort data symbols from the ones with largest power value to the smallest
3- Pass data symbol with largest power value on the subcarrier with higher channel coefficient
$n = n + 1$
endfor

The strategy detailed above is based on the water filling principle in which the signal power is high when the channel SNR is high, and low when the channel SNR is low [**23**]. As a result of this strategy, the more important coding passes experience a better channel condition, and the less important coding passes experience a worse channel condition.

2.7. Simulation Results

We use Kakadu software to encode JPEG2000 images of Lena and Peppers at a size of 512×512, and at a rate of 0.25 bpp; and images of Bridge and Couple both at sizes of 176×144, but at different rates of 0.25 and 0.15 bpp, respectively. The settings for the JPEG2000 codec are 64×64 code-blocks, 128×128 precincts, and one level of decomposition for the sake of simplicity in analysis. The header information is assumed to be transmitted error-free. Binary Phase Shift Keying (BPSK) is used to modulate the bitstream produced by the JPEG2000 encoder. We analyze the performance of the sys-

tem by measuring the average PSNR and the average BER profile of the received image transmitted through multi-tap frequency selective channels. The images are transmitted through a block fading frequency selective channel, and assume that each tap of the channel has a Rayleigh fading distribution with AWGN, and is independent of the other taps. We integrate the OFDM technique with our UPA scheme to eliminate the effect of ISI and ICI, while an optimal amount power is allotted to each transmitting bit. The number of subcarriers (N) used in the OFDM transmitter is 16. The value of N does not have any impact on the performance of the system. However, at higher number of subcarriers, the size of the IFFT and the channel matrix grows linearly, thus the computational complexity of the system increases.

We compare the performance of the UPA-OFDM and Adaptive UPA-OFDM with/without channel aware transmission. Furthermore, we evaluate the PSNR efficiency of our proposals by comparing it with two strategies proposed in [**29**] and [**30**]. The first strategy is a state of the art scheme which protects data against errors by applying different code rates and modulation orders depending on the sensitivity of the layers to channel transmission error. The second strategy presents an energy saving approach to transmission of discrete wavelet transformed images over OFDM channels, based on mapping the important descriptions onto the good channels and discarding the less important ones if the channel is bad.

2.7.1. Performance evaluation of the UPA algorithm in an OFDM system

In Figure 2-15 to Figure 2-18, superior PSNR performance of the system using UPA in contrast with Equal Power Allocation (EPA) is apparent. For example, at a channel SNR value of 20 dB, the UPA algorithm improves the PSNR of the received image of Lena by about 10.5 dB. An assumption in obtaining the average PSNR values in these figures is that the total available power to transmit an image, e_{total}, is fixed. Because employing OFDM increases the amount of the required power (due to the addition of the cyclic prefix), essentially less power will be available to distribute among data bits. This reduction in the amount of power available to data bits in a multi-tap channel reduces the PSNR performance at SNR values lower than 20 dB by less than 1 dB. Theoretically, we can measure this drop by recognizing the amount of extra power required for the cyclic

prefix in 2-tap and 3-tap channels which is equal to $10\log\left(\frac{18}{16}\right) = 0.5$ dB and $10\log\left(\frac{19}{16}\right) = 0.75$ dB, respectively. However, at SNR values of greater than 20 dB, the PSNR performance of the 2-tap and 3-tap channels start to converge, and eventually reach the performance of the non-frequency selective channel. The results also indicate that at very high SNR values, the average PSNR values of the UPA and EPA algorithms approach to each other. This behavior is expected since at high SNR values the bit error rate is very low, regardless of the power allocation algorithm. As expected, if the OFDM technique is not applied to an image transmitted through a frequency selective channel, the average PSNR performance of the received image will have a poor value of about 14.5 dB.

We also compare our results with those of [**29**] and [**30**] for transmission of Lena $(512 \times 512, 0.25)$ bpp over a 2-tap frequency selective channel, in order to evaluate the performance of our proposed UPA-OFDM system. A comparison in Figure 2-15 indicates that our proposal surpasses the results of Dardari *et al*. in [**29**] by about 10 dB at all SNR values. Furthermore, our proposal maintains a higher data rate than that of [**29**] because we have not considered forward error correction coding. In [**30**], Sharma *et al*. validate their simulation results at SNR values of 15 dB and 20 dB for different power threshold values. They vary the power threshold at the transmitter based on the severity of the subchannels. The more severe is the channel; the lower is the power threshold, thus less number of descriptions is discarded at the transmitter. At SNR values of 15 dB and 20 dB, our proposal has 1 dB to 5 dB gain advantage over the proposal of [**30**] if their power threshold is set lower than 7 dB or higher than 12 dB. For the values in between, where the channel has a moderate condition, proposal of [**30**] surpasses the PSNR performance of our proposal by a maximum value of 3 dB. That is, the strategy in [**30**] performs better than our proposal only at particular channel behaviour for which they can set a specific power threshold.

Figure 2-19 to Figure 2-22 show the BER performance of the received bitstream of the images. The impact of having less power available to assign to data bits in a multi-tap channel, due to addition of cyclic prefix, can be seen here as well. An interesting observation on these figures is that for SNR values less than 15 dB the EPA scheme has a lower BER than the UPA algorithm. However, as shown in Figure 2-15 to Figure 2-18,

the PSNR performance when employing the UPA algorithm is much higher in comparison with the EPA technique. Moreover, although the 2^{nd} scenario without OFDM demonstrates a low PSNR value of 14.5 dB regardless of the SNR value, yet its BER performance shows an improving trend as SNR increases up to 16 dB, and beyond that, an error flow occurs.

The explanation lies in the fact that the BER curves show the average probability of any information bit being received with error, regardless of its location in the JPEG2000 bitstream and its impact on the distortion (equivalently on the PSNR) of the received image. For the UPA algorithm, bits with low impact in the distortion are protected much less than the bits with high impact. This results in a high overall BER for this scenario; however, the distortion in the received image is lower compared to the EPA case, simply because bits with higher impact in the distortion are received at a much lower error rate. As a result, the BER profile is not a reliable metric on its own to measure quality of the received images.

Another observation on Figure 2-19 and Figure 2-22 is the abrupt fall of the BER curve between SNR values of 14 and 16 dB. The reason is that, between SNR values of 0 to 14 dB, the UPA algorithm has a preference to set the power of some less important coding passes to zero in order to minimize the distortion of the received image. This obviously results in a BER of 50% for bits with zero power and consequently a higher BER averaged over all bits. As SNR increases to 14 dB, less number of coding passes possesses zero power, and eventually at SNR of 16 dB and higher, all coding passes are assigned power values greater than zero.

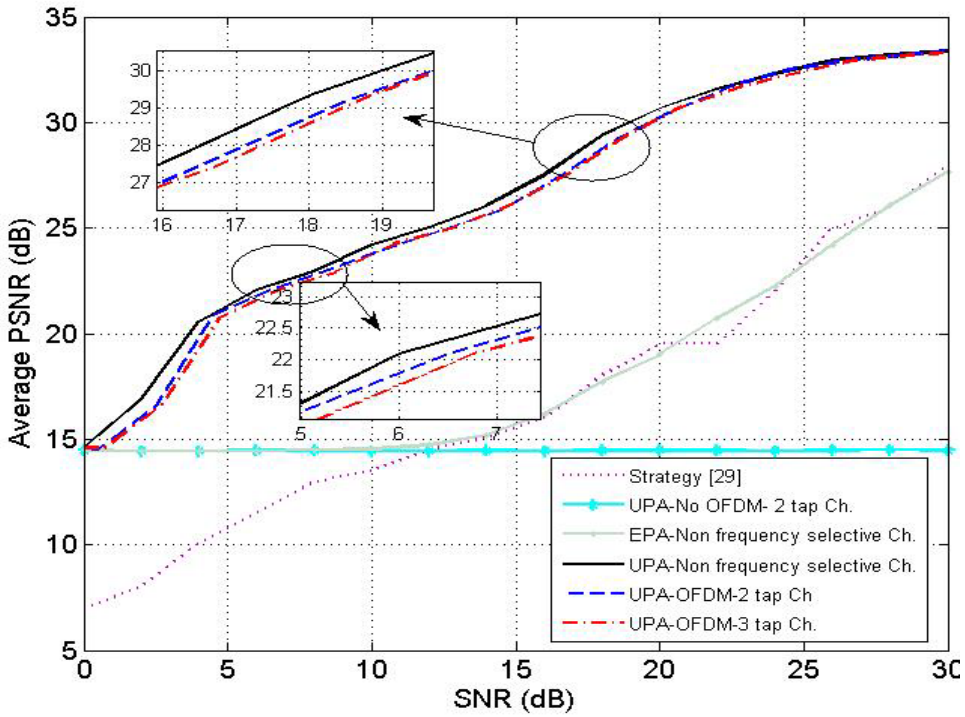

Figure 2-15: Comparison and evaluation of the PSNR of the received Lena $(512 \times 512, 0.25$ ***bpp) in the UPA-OFDM system***

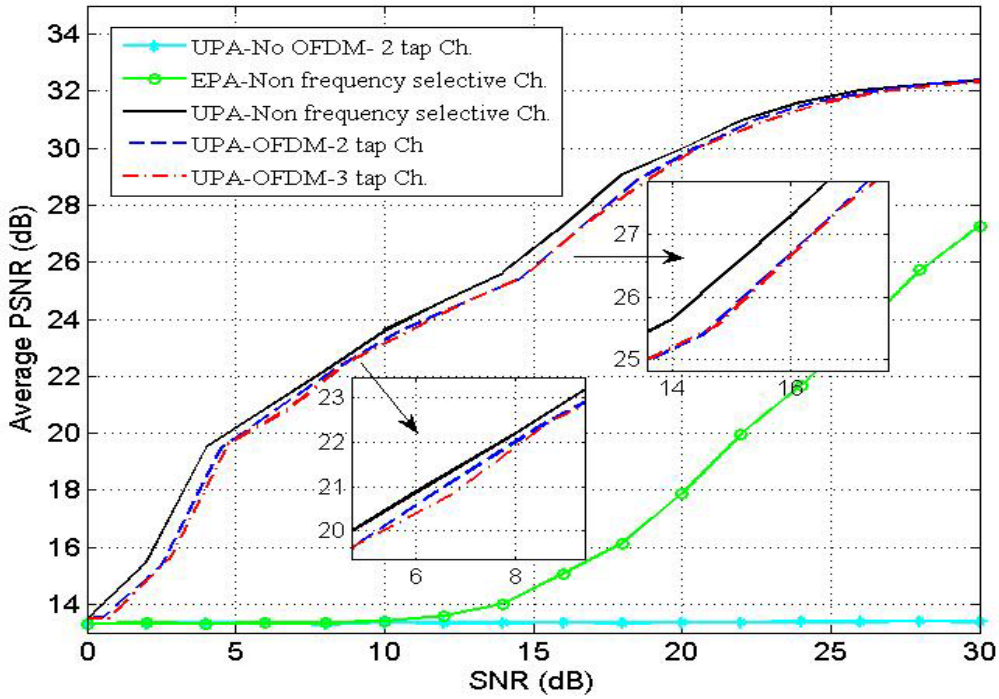

Figure 2-16: Comparison of the PSNR of the received Peppers ($512 \times 512, 0.25$ ***bpp) in the UPA-OFDM system***

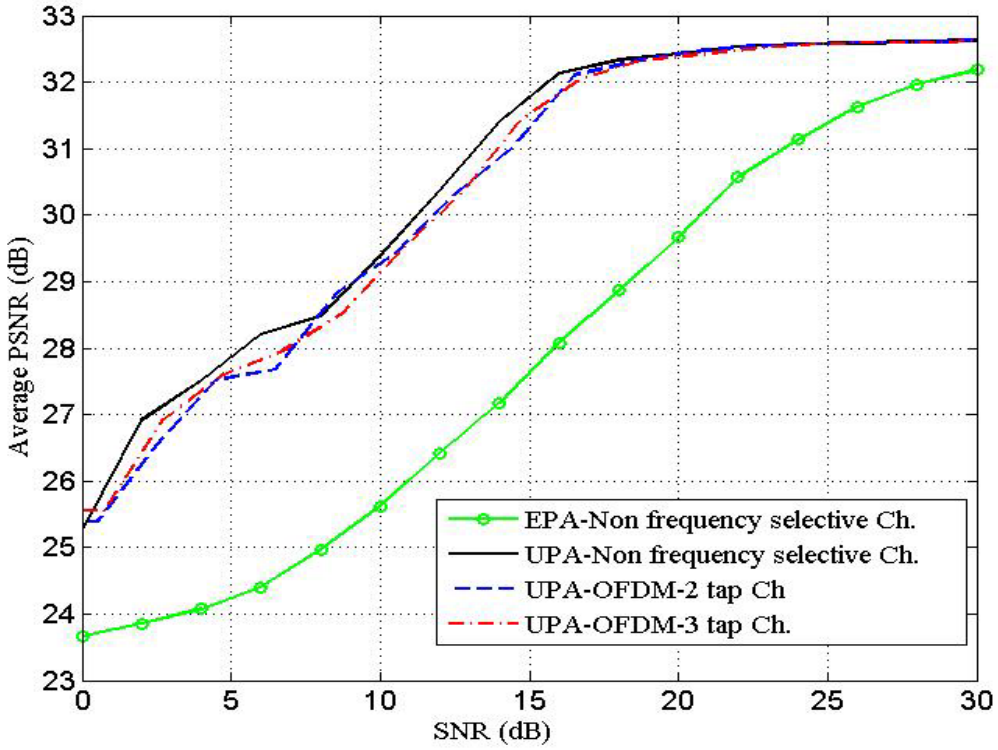

Figure 2-17: Comparison of the PSNR of the received Bridge ($176 \times 144, 0.25$ ***bpp) in the UPA-OFDM system***

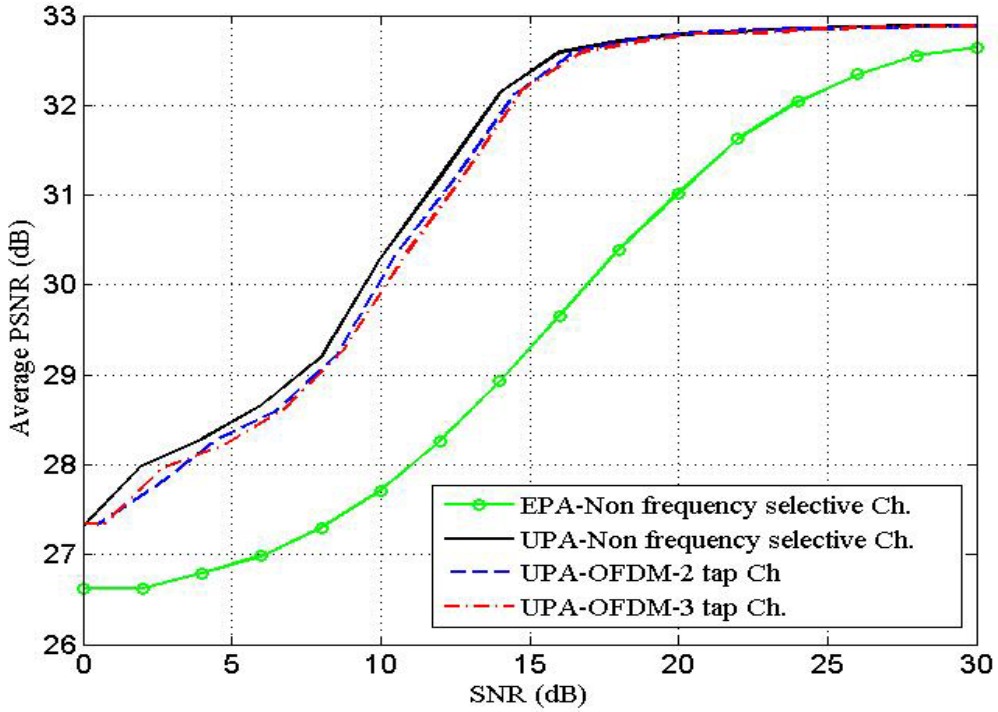

Figure 2-18: Comparison of the PSNR of the received Couple ($176 \times 144, 0.15$ ***bpp) in the UPA-OFDM system***

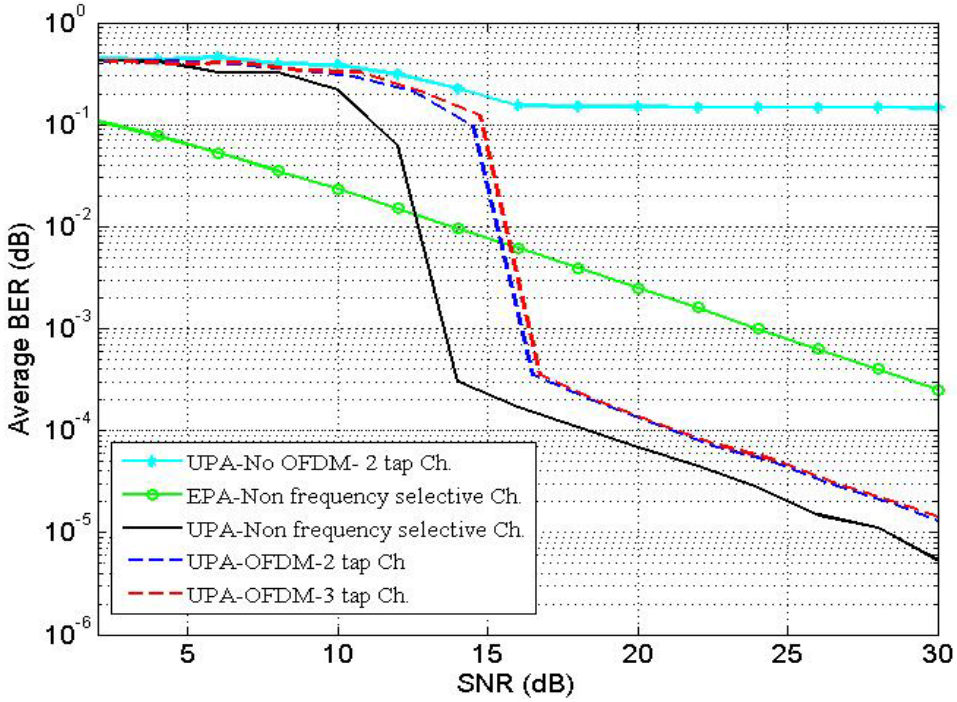

Figure 2-19: Comparison of the BER of the received Lena $(512 \times 512, 0.25\ bpp)$ ***in the UPA-OFDM system***

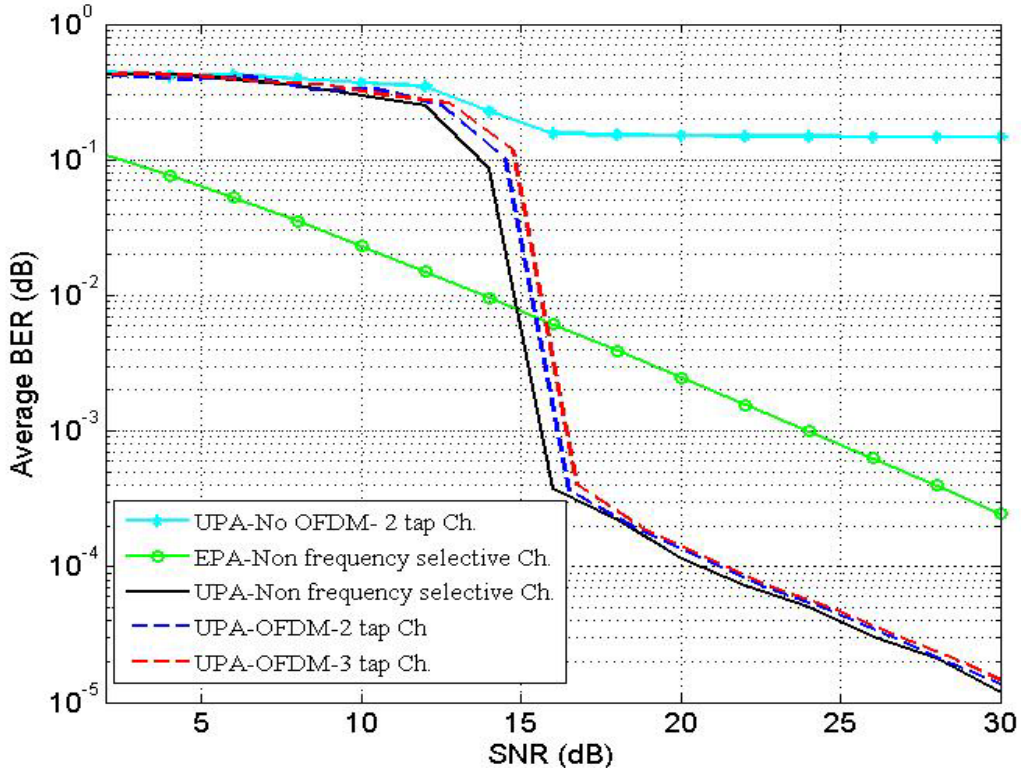

Figure 2-20: Comparison of the BER of the received Peppers $(512 \times 512, 0.25\ bpp)$ ***in the UPA-OFDM system***

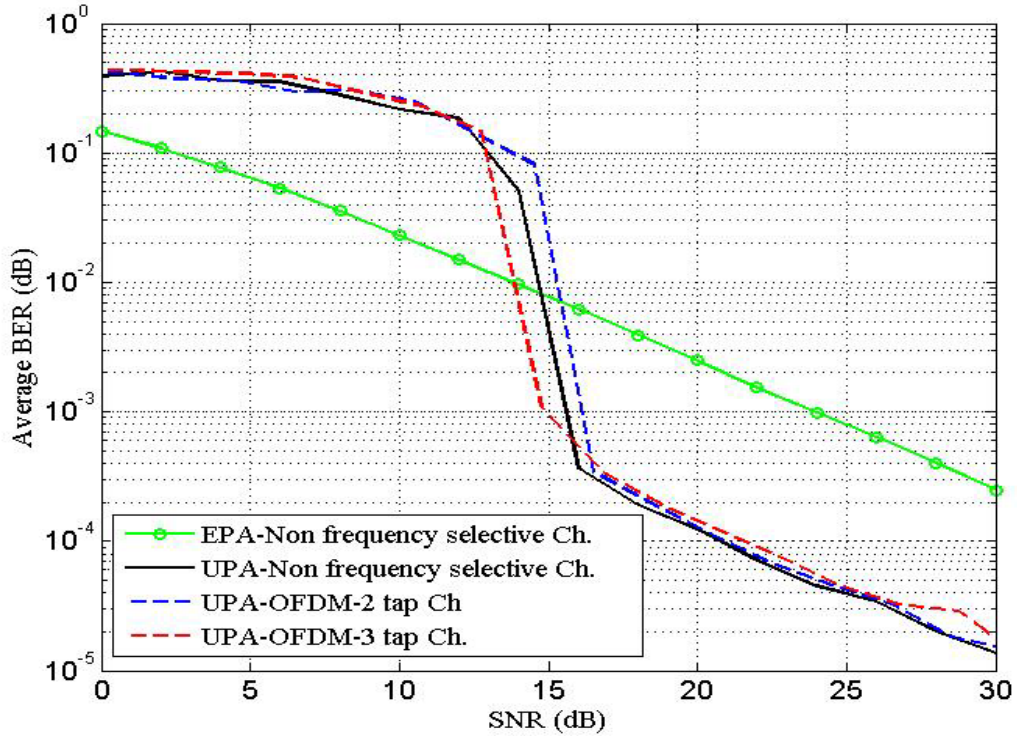

Figure 2-21: Comparison of the BER of the received Bridge $(176 \times 144, 0.25\ bpp)$ ***in the UPA-OFDM system***

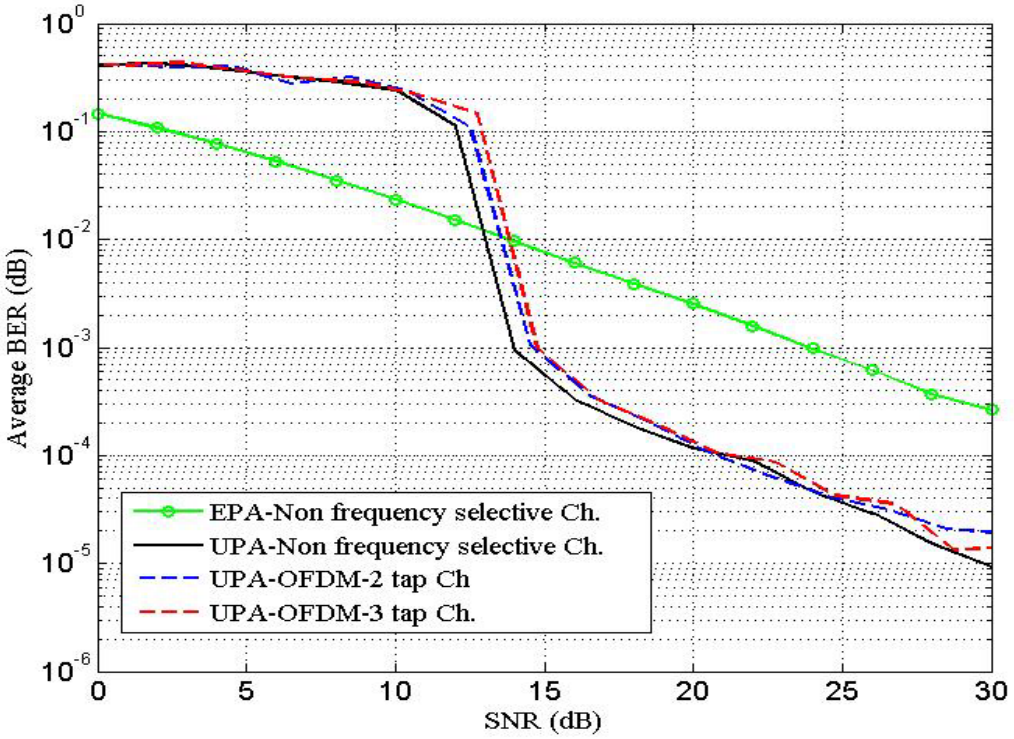

Figure 2-22: Comparison of the BER of the received Couple $(176 \times 144, 0.15\ bpp)$ ***in the UPA-OFDM system***

2.7.2. Performance Evaluation of the Adaptive UPA scheme in an OFDM System

To realize the impact of our proposed adaptive UPA technique with channel assignment strategy on the quality of the received image, we analyze the performance of the system by transmitting 1000 images of Lena and Peppers ($512 \times 512, 0.25$ bpp) through Block fading and 3-tap frequency selective channels. The benchmark for the simulations in this section is the PSNR profile of the received images transmitted over block fading non-frequency selective channel with UPA algorithm. We also apply the channel assignment strategy to our UPA-OFDM algorithm in order to achieve fairness in the simulation comparisons.

Figure 2-23 demonstrates that our channel assignment strategy contributes to an overall improvement in the quality of the received image. To obtain the average PSNR values, we assume that the total available power to transmit an image (e_{total}) is fixed. Due to addition of the cyclic prefixes in the OFDM symbols, essentially less amount of power will be available to distribute among data bits. This reduction in the available power to the data bits transmitted through a multi-tap channel results to a reduction of the PSNR performance at SNR values less than 20 dB. Figure 2-23 shows that our channel assignment strategy is more effective on the mid-range SNR values between 11 dB and 18 dB, where the PSNR performance is improved by 0.2 dB. This figure also reveals the advantage of employing the proposed adaptive scheme along with the channel assignment strategy for frequency selective channels at very low and mid-range SNR values. The adaptive scheme succeeds to completely compensate for the PSNR reduction in frequency selective channels at the SNR values of 2 dB and between 12 dB and 14 dB. For SNR values between 0 dB to 4 dB and 12 dB to 20 dB, integration of the adaptive scheme and the channel assignment strategy yields a PSNR improvement of about 1 dB and 0.5 dB, respectively.

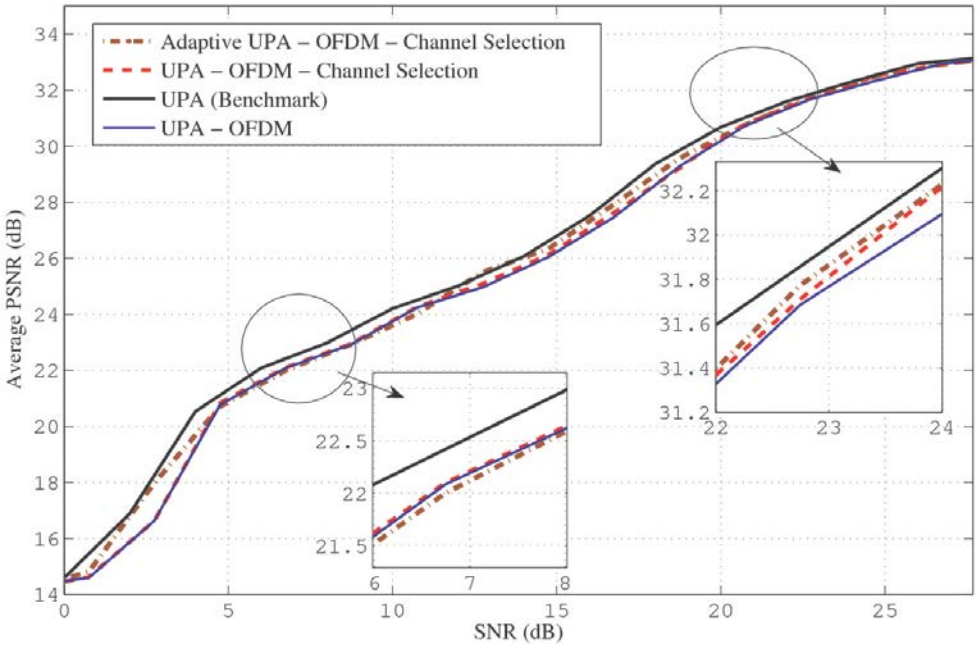

Figure 2-23: Evaluation of PSNR value of the received Lena $(512 \times 512, 0.25\ bpp)$ ***in Adaptive UPA-OFDM system***

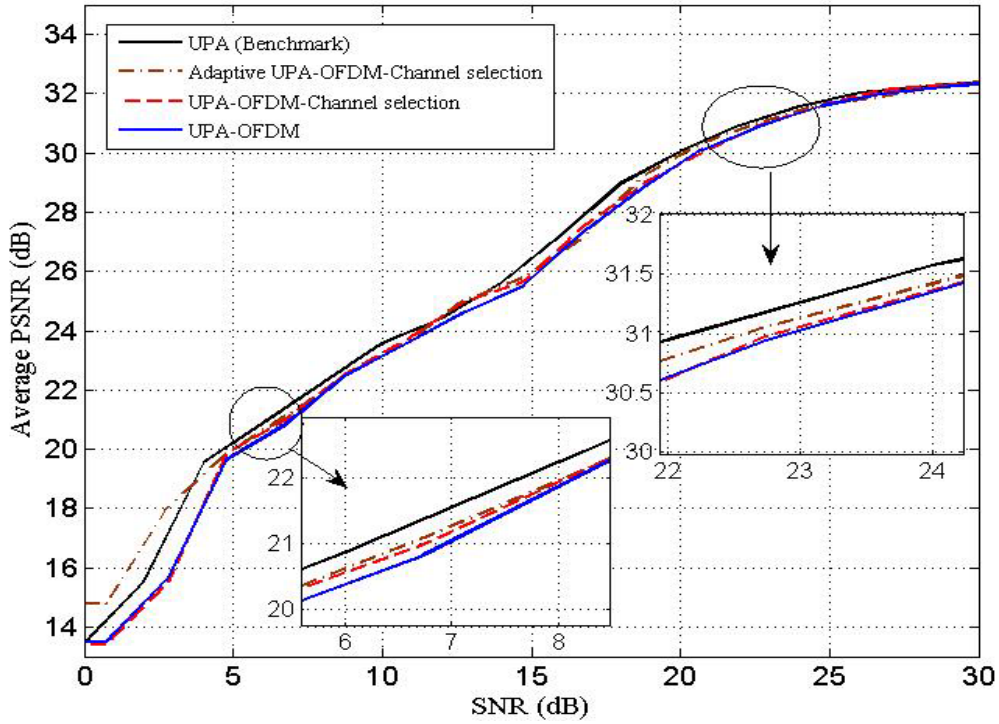

Figure 2-24: Evaluation of PSNR value of the received Peppers $(512 \times 512, 0.25\ bpp)$ ***in Adaptive UPA-OFDM system***

2.7.3. Visual Comparison of the Proposed methodologies

In this section, we present a visual comparison between our proposed UPA, UPA-OFDM, and adaptive UPA-OFDM, with/without channel aware transmission. The received images of Lena and Peppers are transmitted at an SNR value of 16 dB over block fading frequency selective channels.

Figure 2-25 to Figure 2-28 present a visual comparison for transmission of "Lena" and "Peppers" in which the UPA technique is applied on the images transmitted through scenarios tabulated in Table 2-4. Note that the visual quality of the received images is enhanced when UPA algorithm is applied; and as the number of channel taps increases, slight degradation in the visual quality of the received image is noticeable. These figures also indicate that the visual qualities of the received images are enhanced when the channel assignment strategy is applied. In addition, utilization of the adaptive scheme improves noticeably the visual quality of the received image.

Table 2-4: Transmission scenarios in the UPA-SCFDE system (SNR=16 dB)

Scenario	**Transmission Scenario**	**PSNR (dB)**			
		Lena	Peppers	Bridge	Couple
(a)	Original Image	------	-------	-------	--------
(b)	Using UPA over non-frequency selective channel	27.99	27.22	32.14	32.80
(c)	Using UPA& OFDM over 2-tap frequency selective channel	26.77	26.75	31.75	32.59
(d)	Using UPA& OFDM over 3-tap frequency selective channel	26.75	26.49	31.45	32.22
(e)	Using UPA & OFDM & Channel assignment strategy over 3-tap frequency selective channel	26.86	26.61	31.55	32.58
(f)	Using Adaptive UPA & OFDM & Channel assignment strategy over 3-tap frequency selective channel	27.05	26.81	32.10	32.72

(a) (b)

(c) (d)

(e) (f)

Figure 2-25: Visual comparison of "Lena" at 512×512, 0.25 bpp, transmitted at SNR=16 dB over the scenarios in Table 3-4

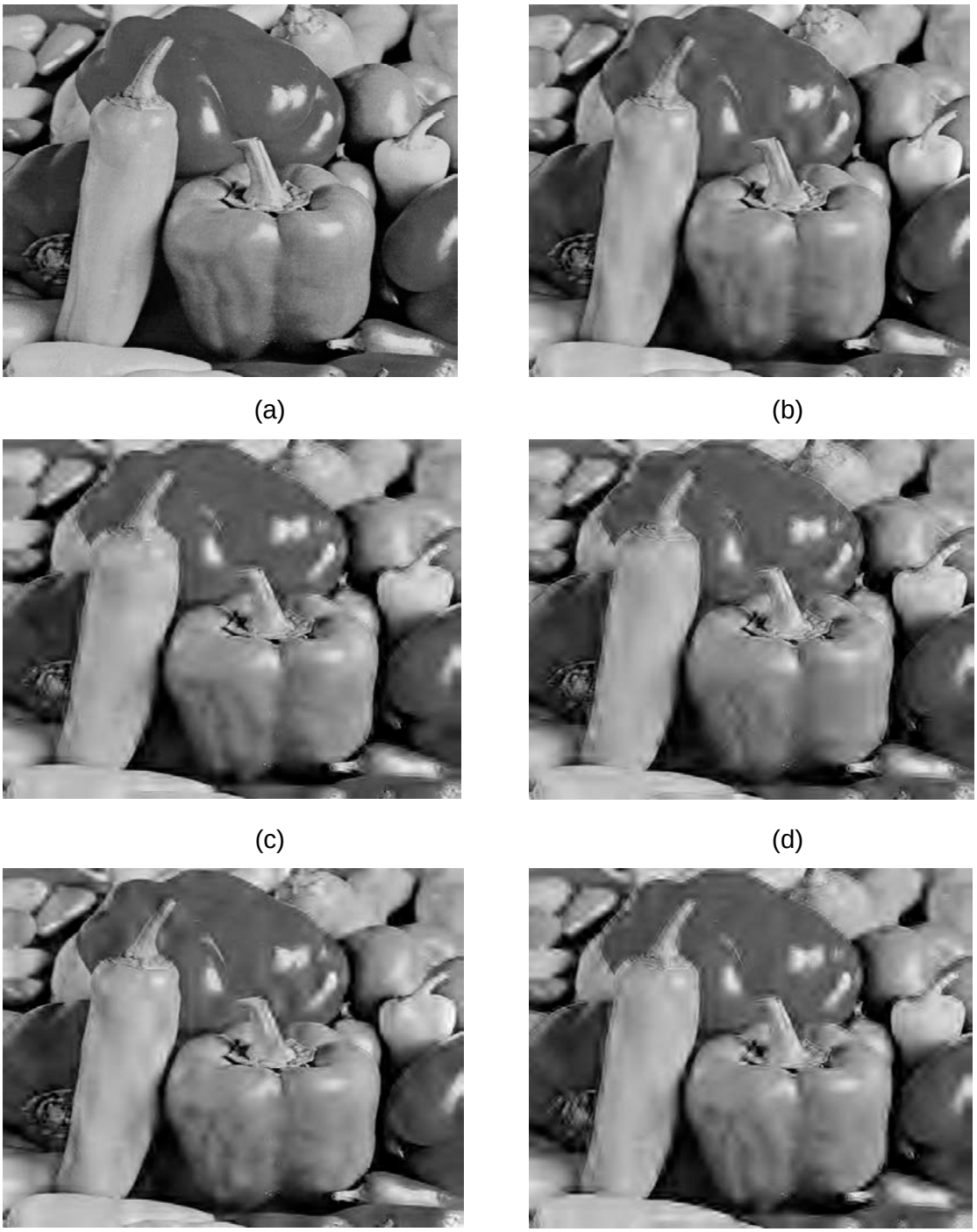

(a) (b)

(c) (d)

(e) (f)

Figure 2-26: Visual comparison of "Peppers" at 512×512, 0.25 bpp, transmitted at SNR=16 dB over the scenarios in Table 3-4

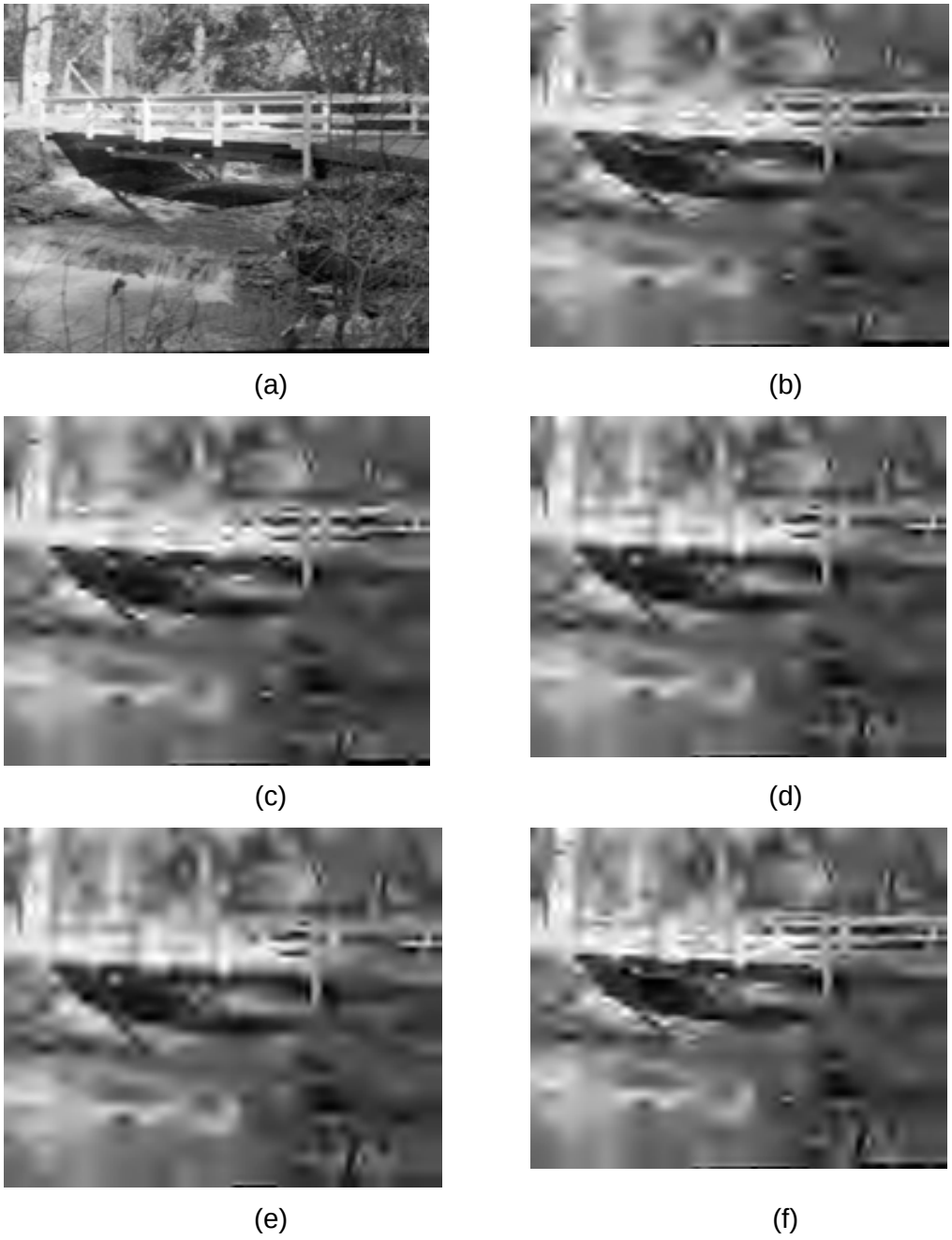

(a) (b)

(c) (d)

(e) (f)

Figure 2-27: Visual comparison of "Bridge" at 176×144, 0.25 bpp, transmitted at SNR=16 dB over the scenarios in Table 3-4

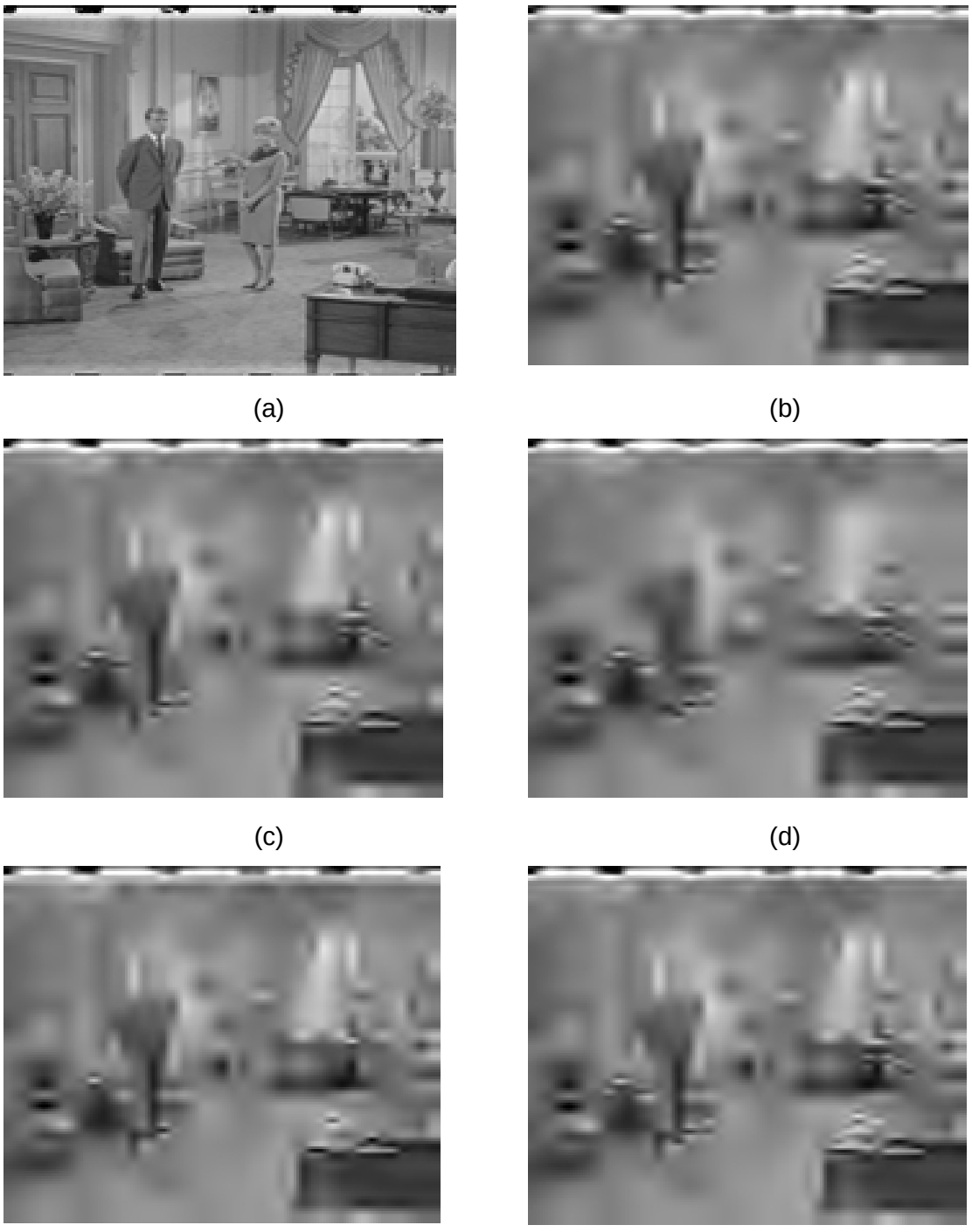

(a) (b)

(c) (d)

(e) (f)

Figure 2-28: Visual comparison of "Couple" at 176×144, 0.15 bpp, transmitted at SNR=16 dB over the scenarios in Table 3-4

2.8. Summary

This chapter discusses transmission of JPEG2000 images through frequency selective block fading channels using an UPA algorithm and OFDM technique. The UPA optimization algorithm (proposed in [**25**]) allocates unequal power to each coding pass based on its contribution to the quality of the received image. We also develop an adaptive scheme within the UPA algorithm in order to allow variable size groups in the process of optimal power allocation over the coding passes. At any SNR value, we determine the appropriate number of group which results into an enhanced quality of the received image. In addition, a new channel assignment strategy is introduced to the OFDM transmitter of the system, where the more important coding passes are transmitted over the subcarriers with higher channel gain.

The simulation results for "Lena", "Peppers", “Bridge”, and “Couple” images confirm that employing the UPA algorithm over EPA technique improves the PSNR performance for non-frequency selective channels by as much as 10.5 dB at SNR value of 20 dB. Our integrated OFDM and UPA system maintains this superior performance for frequency selective channels. This system removes the negative effects of ISI and ICI; however, slight degradation in the PSNR performance is noticeable. The loss in the performance is about 0.5 dB at SNR value of 7 dB for a 2-tap channel. Nevertheless, the system eliminates this degradation in performance at SNR values higher than 25 dB, in which the system exhibits a PSNR performance as if the images are transmitted over non-frequency selective channels. Moreover, the BER performance of the received images is analyzed for different scenarios where UPA, EPA and OFDM are applied. The results indicates that even though the UPA scheme surpasses the EPA technique in PSNR performance for all SNR values, but the BER curve of the EPA technique exhibits lower values than the BER curve of the UPA scheme for SNR values less than 15 dB. To establish that our proposed system preserves power constraint of the optimization problem, the total actual amount of power consumed for transmission of Lena ($512 \times 512, 0.25$bpp) is measured and revealed that it matches the total available power originally assumed at the transmitter, with a close precision.

The simulation results for incorporating the proposed adaptive scheme within the UPA algorithm prove an improvement of the PSNR performance of the system up to 2.5

dB for the SNR values between 0 dB and 20 dB. This improvement can be achieved either as an increase in the PSNR of the received image or as an energy conservation if the same quality is maintained. Simulation results also demonstrate that the channel assignment strategy enhances the PSNR performance of the received image up to 0.2 dB. Integration of the proposed adaptive scheme with the channel assignment strategy leads to a gain advantage of up to 1 dB and 0.5 dB at low end and mid band SNR values, respectively.

This chapter is the result of works published in [**31**] and [**32**].

3. Chapter 3: Comparison of Single-Carrier Transmission of JPEG2000 Images with Multi-Carrier Transmission

3.1. Transmission of JPEG2000 Images with UPA over Single Carrier Transmission Systems

OFDM is a multicarrier communication technique that has attracted the interests of the academic and industrial communities in the resent years. In wire line communications, OFDM has been employed by several standards such as the High-bit-rate Digital Subcarrier Line (HDSL) and Very-high-speed Digital Subcarrier Line. In wireless systems, it has been used by the Digital Audio Broadcasting (DAB), Digital Video Broadcasting for Terrestrial Television (DVB-T) and Wireless Local Area Networks (WLANs), which are based on the IEEE 802.11 standards

Unfortunately, OFDM has the drawback of high Peak to Average Power Ratio (PAPR). As an attractive alternative to Multi-Carrier (MC) techniques, Cyclic Prefixed Single-Carrier (CP-SC) transmission techniques have recently attracted considerable attention due to their low PAPR. In practice, OFDM is implemented in the base station of a cellular network for downlink data transmissions, and Single Carrier Frequency Domain Equalization (SCFDE) is adapted at the end user station for uplink data transmissions [**2**].

To our best knowledge, most, if not all, of the literature reports on multimedia data transmission over frequency selective channels, with UEP or UPA, utilize the OFDM technique to combat the negative impact of ISI and ICI. This chapter integrates our UPA algorithm with SCFDE to provide protection for uplink transmission of JPEG2000 coded bitstreams in block fading frequency selective channels. Moreover, our SCFDE system

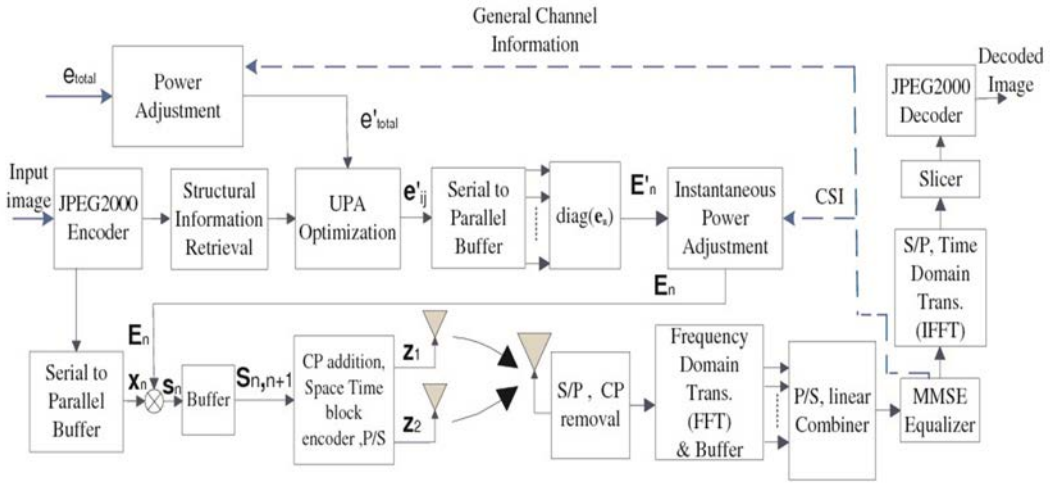

Figure 3-1: SCFDE system model

obtains spatial and multipath diversity during transmission by using Alamouti's Space Time Block Coding (STBC) scheme [**22**] and MMSE frequency domain equalization, respectively.

3.1.1. System Model

The overall system block diagram is presented in Figure 3-1. Chapter 2 explains about the functionality of the UPA optimization algorithm, the structural information retrieval unit, and the power adjustment unit. As revealed in Section 2.5, the UPA optimization unit assumes an AWGN channel for the transmission medium. The fading impact of the channel is taken into consideration in the Instantaneous Power Adjustment unit by altering the amount of power allocated to each coding pass by the UPA algorithm. Section 3.1.2 will describe the functionality of the power adjustment unit for the SCFDE system. The bitstream and the power assigned to each bit are categorized into N_B blocks. Before the transmission, every block of data is appended with a cyclic prefix, and every two consecutive blocks, i.e, n^{th} and $(n+1)^{\text{th}}$, are Alamouti coded, where $(n = 1, 2, \dots, N_B)$.

The two transmit antennas model exploit spatial diversity which increases the reliability of the wireless link and improves the quality of the received image. This model improves the quality of the received image without increasing the transmit power. Thus,

the two transmit antenna system is capable of conserving more energy than the single transmit antenna system.

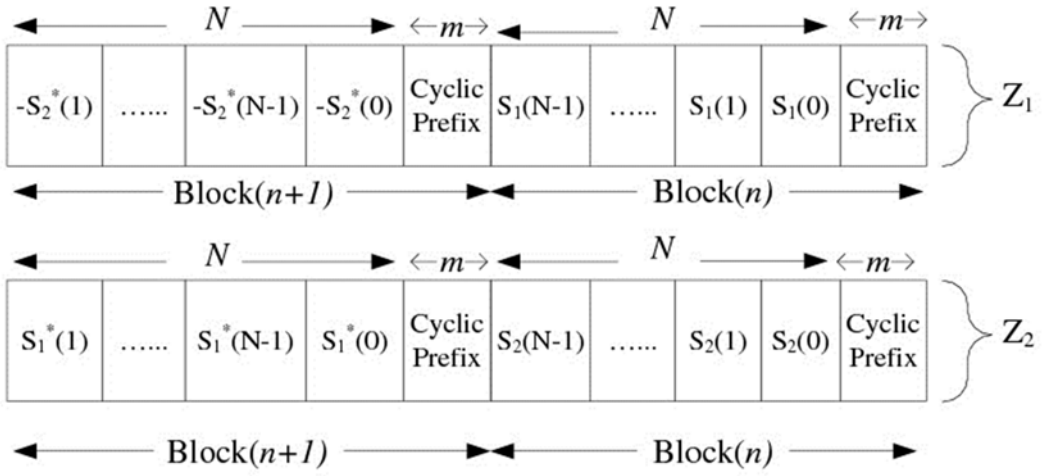

Figure 3-2: Transmission block format for SCFDE-STBC [33]

The channel impulse response between the j^{th} transmitter antenna and the receiver, for the n^{th} transmission block is given by $\mathbf{h}_{n,j} = [h_0, h_1, \dots, h_{m-1}]^T$**,** where m is the channel memory length. The beginning of each data block, with a size of $N \times 1$, is appended with the last m samples of the same block, to eliminate the impact of ISI and to form the channel matrix circulant. At the receiver side, the first m samples of every block are discarded and only N samples are processed. Forming the channel into a circulant matrix accounts for the addition and removal of the cyclic prefixes for every n^{th} transmission block.

FDE-STBC was suggested in [**33**] as an extension of Alamouti scheme [**22**] to frequency selective channels by imposing the Alamouti orthogonal structure at a block level, rather than the original symbol-level implementation used for frequency-flat fading channels. Following [**33**], the transmitted blocks over the first and the second antenna are generated according to the encoding rule presented in Figure 3-2. Denote in this figure, $\boldsymbol{S}_n = \sqrt{\boldsymbol{E}_n}\mathbf{x}_n$, and $\boldsymbol{S}_n = [s_0,\ s_1, \dots, s_{N-1}]$**,** and the n^{th} transmitted block from antenna j by $\boldsymbol{S}_{n,j}(i)$**.** At times $n = 0, 2, 4, \dots$, pairs of length-N blocks $\boldsymbol{S}_{n,1}(i)$ and $\boldsymbol{S}_{n,2}(i)$ (for $i =$

$0, 1, \dots, N-1$) are generated by an information source with the following transmit diversity scheme [**33**]:

$$\begin{aligned} \boldsymbol{S}_{n+1,1}(i) &= -\boldsymbol{S}_{n,2}^{*}((-i)_{\boldsymbol{N}}) \ , \qquad i = 0, 1, \dots, N-1 \\ \boldsymbol{S}_{n+1,2}(i) &= \boldsymbol{S}_{n,1}^{*}((-i)_{\boldsymbol{N}}) \ , \qquad n = 0, 2, 4, \dots \end{aligned} \tag{3-1}$$

where $(.)^{*}$ and $(.)_{N}$ denote complex conjugation and modulo-N operations, respectively. The received signal in the first and the second time slots at the receiver side are given by:

$$\begin{aligned} \mathbf{r}_{n_1} &= \mathbf{H}_{n,1}\sqrt{\mathbf{E}_{n,1}}\mathbf{x}_{n,1} + \mathbf{H}_{n,2}\sqrt{\mathbf{E}_{n,2}}\mathbf{x}_{n,2} + \mathbf{v}_{n_1} \ , \\ \mathbf{r}_{n_2} &= -\mathbf{H}_{n,1}\sqrt{\mathbf{E}_{n,2}}\mathbf{x}_{n,2}^{*} + \mathbf{H}_{n,2}\sqrt{\mathbf{E}_{n,1}}\mathbf{x}_{n,1}^{*} + \mathbf{v}_{n_2} \ , \end{aligned} \tag{3-2}$$

where $\mathbf{r}_{n_1}$ and $\mathbf{r}_{n_2}$are the received signal of the n^{th} transmission block at the first and second time slot, respectively. $\mathbf{H}_{n,1}$ and $\mathbf{H}_{n,2}$ are circulant matrices, with entries $\left[\mathbf{H}_{n,j}\right]_{ik} = \left[\mathbf{h}_{n,j}\right]_{(i-k)\ mod\ N}$, $\left[\mathbf{h}_{n,j}\right]_{i} = 0$ for $i > m-1$, $j = 1, 2$, and they represent the CIR of the first and the second antenna, respectively. $\mathbf{v}_{n_1}$ and $\mathbf{v}_{n_2}$ symbolize the AWGN vector of mean zero and variance of $\frac{1}{2}$ per dimension for the first and second time slot, respectively. $\mathbf{E}_{n,1}$ and $\mathbf{E}_{n,2}$ are the actual power values of the n^{th} block of data ($\mathbf{x}_{n,1}$ and $\mathbf{x}_{n,2}$) transmitted from the first and second transmission antenna, respectively. Equation (3-6) formulates the calculation of the actual power of each bit from the assigned valued by the UPA optimization algorithm. The available power for transmission at any of the two antennas is half of the values in the single transmission antenna case, in order to keep the total transmit power constant.

The received signal is converted into frequency domain by multiplying by the FFT matrix as follows [**33**]:

$$\begin{aligned} \mathbf{c}_{n_1} &= \Lambda_{n,1}\mathbf{Q}\sqrt{\mathbf{E}_{n,1}}\mathbf{x}_{n,1} + \Lambda_{n,2}\mathbf{Q}\sqrt{\mathbf{E}_{n,2}}\mathbf{x}_{n,2} + \mathbf{Q}\mathbf{v}_{n_1} \ , \\ \mathbf{c}_{n_2} &= -\Lambda_{n,1}\mathbf{Q}\sqrt{\mathbf{E}_{n,2}}\mathbf{x}_{n,2}^{*} + \Lambda_{n,2}\mathbf{Q}\sqrt{\mathbf{E}_{n,1}}\mathbf{x}_{n,1}^{*} + \mathbf{Q}\mathbf{v}_{n_2} \ , \end{aligned} \tag{3-3}$$

where $\mathbf{c}_{n_1} = \mathbf{Q}\mathbf{r}_{n_1}$ and $\mathbf{c}_{n_2} = \mathbf{Q}\mathbf{r}_{n_2}$.The next step is to perform a linear combining as follows:

$$\hat{\mathbf{r}}_{n,1} = \Lambda_{n,1}^{*}\mathbf{c}_{n_1} + \Lambda_{n,2}\mathbf{c}_{n_2}^{*} \ ,$$
$$\hat{\mathbf{r}}_{n,2} = \Lambda_{n,2}^{*}\mathbf{c}_{n_1} - \Lambda_{n,1}\mathbf{c}_{n_2}^{*} \ . \tag{3-4}$$

The received data in (3-4) are time reversed according to the encoding rule in ure 3-2. Then, the receiver uses a diagonal matrix ($\mathbf{W}$) of size $N \times N$ to perform an MMSE equalization on the resulting signals in (3-4) which are in frequency domain. The elements of the equalizer matrix are given by [**33**]:

$$[\mathbf{W}_n]_{ii} = \frac{1}{\left|\left[\Lambda_{n,1}\right]_{ii}\right|^2 + \left|\left[\Lambda_{n,2}\right]_{ii}\right|^2 + \frac{1}{SNR}} \ , \tag{3-5}$$

where SNR stands for Signal to Noise Ratio. This equalizer can be used for the signals received at both time intervals. The output of the MMSE equalizer will be $\hat{\mathbf{y}}_n = \mathbf{W}_n\hat{\mathbf{r}}_n$, where $\hat{\mathbf{r}}_n$ is the output of the linear combiner. Next, The output of the equalizer is transferred into time domain by applying the IFFT to recover the original data given by $\hat{\mathbf{s}}_n = \mathbf{Q}^H\hat{\mathbf{y}}_n$, where $(.)^H$ denotes complex conjugate transpose operation. At the end, the receiver applies a hard decision slicer on the recovered data, and passes it to the JPEG2000 decoder to generate the received image.

3.1.2. Instantaneous Power Adjustment Unit

As we previously explained, the UPA algorithm in [**9**] assumes an AWGN channel at the time of power allocation to the coding passes. The Instantaneous Power Adjustment unit compensates for the effect of fading before transmission by using the instantaneous values of the channel impulse response. The compensation for the effect of fading in a multi-transmission antenna channel is given by:

$$\mathbf{E}_{n,j} = \frac{\acute{\mathbf{E}}_{n,j}}{\alpha + \sum_0^{m-1}|h_k|^2} \ , \tag{3-6}$$

where h_k is the k^{th} channel tap for the n^{th} transmission block and m is the channel memory length or the total number of taps. $\acute{\mathbf{E}}_n$ is the assigned power to the bits within the n^{th} transmission block by the UPA optimization algorithm, and $\mathbf{E}_n$ represents the corresponding power of the bits after the effect of channel fading is taken into consideration.

3.2. Comparison of OFDM and MMSE-SCFDE over Frequency Selective Channels

Many researchers consider progressive image transmission in OFDM systems, and few evaluate the transmission of images in single carrier systems in the literature. A comparison between OFDM and SCFDE needs to be undertaken to investigate their different behaviors in transmission of JPEG2000 images in single antenna and multiple-input multiple-output systems, and how much these two techniques are capable of conserving bandwidth at different source coding rates. Also, an important criterion in designing a system for wireless image transmission is to maintain a low complexity in order to avoid time delay in coding and transmission, and reduce the fabrication cost.

This section investigates and compares the PSNR performance of the Linear Constellation Pre-Coding (LCP) OFDM and MMSE-SCFDE systems for the transmission of JPEG2000 images over frequency selective channels. For the sake of comparison, we consider EPA to distribute the available power over the coding passes. Finally, this section examines the amount of bandwidth conservation that these two systems can provide either in the case of single transmission antenna or multiple transmission antennas, by measuring the PSNR of the received image at different bit budgets.

3.2.1. System Model

Figure 3-3 and Figure 3-4 present our proposed block diagrams which use SCFDE and OFDM, respectively. Yue *et al*. propose a transmission model for integrating STBC as an inner code with OFDM to achieve diversity gain in [**34**]. This section uses the proposals of [**33**] and [**34**] to integrate STBC with MMSE-SCFDE and LCP-OFDM, respectively, for wireless image transmission. In Chapter 2 , we have demonstrated that the OFDM technique is not able to achieve multipath diversity, and the PSNR performance of a received image from a frequency selective channel in an OFDM system deteriorates as the number of channel taps increases. A similar trend for a SCFDE system has been demonstrated in Section 3.1, where we have measured lower PSNR values at higher number of channel taps. In both of these studies, our proposals included integration of OFDM and SCDDE with an optimized unequal power allocation algorithm. In this section, our proposal allocates an equal amount of power on codestream of an image to

establish a fair comparison between LCP-OFDM and SCFDE for wireless image transmission.

The LCP technique can be used to obtain multipath diversity in an OFDM system. The multipath diversity enhances the quality of the received signal at higher number of channel taps [**35**]. In this technique, the symbols are pre-coded at the transmitter with a linear constellation matrix. The pre-coder matrix (**θ**) is unitary, as a result it neither increases power nor reduces the transmission rate. This matrix is represented by a Vandermonde matrix as follows [**35**]:

$$\boldsymbol{\theta} = \frac{1}{\beta}\begin{pmatrix} 1 & \alpha_1 & \dots & \alpha_1^{N-1} \\ 1 & \alpha_2 & \dots & \alpha_2^{N-1} \\ \vdots & \vdots & & \vdots \\ 1 & \alpha_N & \dots & \alpha_N^{N-1} \end{pmatrix}, \tag{3-7}$$

where N is the number of subcarriers, and β is a normalization factor to impose the power constraint $\mathrm{tr}(\boldsymbol{\theta}\boldsymbol{\theta}^H) = N$, with tr(.) denoting matrix trace. $\{\alpha_N\}_{n=1}^{N}$ are the roots of $x^n - \sqrt{-1} = 0$, if n is a power two. In our analysis, we consider power of 2 values for N, albeit in [**35**] design of the LCP matrix for different values of N is explained. At the receiver side, inverse of the LCP matrix ($\boldsymbol{\theta}^{-1}$) is used to compensate for the pre-coding. Detailed algebraic derivation of constructing this matrix is available in [**36**].

On the transmitter side of the systems, the JPEG2000 encoder transforms the format of an input image into JPEG2000 format and generates a scalable coded bitstream. The OFDM system performs a multicarrier modulation (i.e, multiplying by the IFFT matrix) at the transmitter; however, the transmitter model in the SCFDE system does not include any Fourier transformation. This approach not only reduces the computational complexity in the SCFDE transmitter terminal, but also leads to a lower PAPR as compared with OFDM. The multicarrier implementation of OFDM technique leads to a large PAPR and high sensitivity to carrier frequency offsets. To tackle these issues, OFDM can be implemented in the base station of a cellular network for down-link data transmissions, and SCFDE is adapted at the end user station for uplink data transmissions [**2**].

The channel model and its circulant structure have been discussed in Chapter 2 and Section 3.1.1. Here, we consider similar channel model and review our assumptions

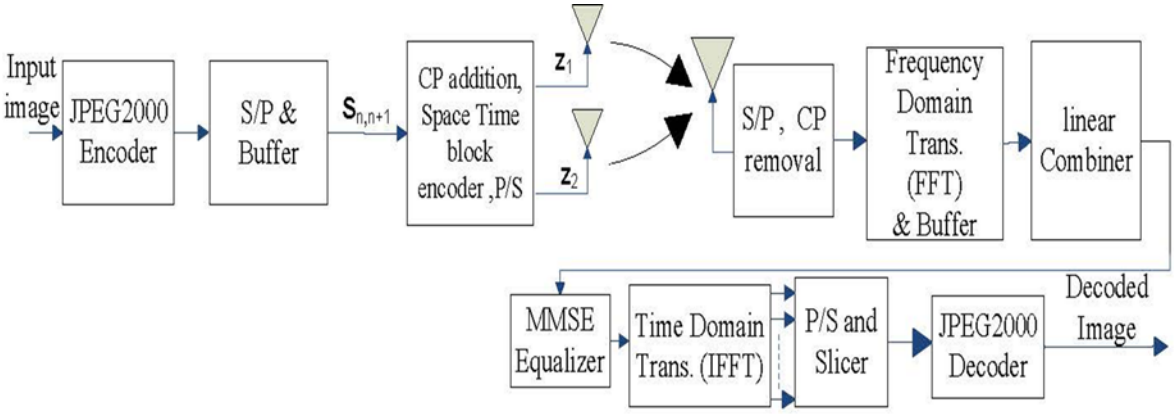

Figure 3-3: SCFDE system model with EPA

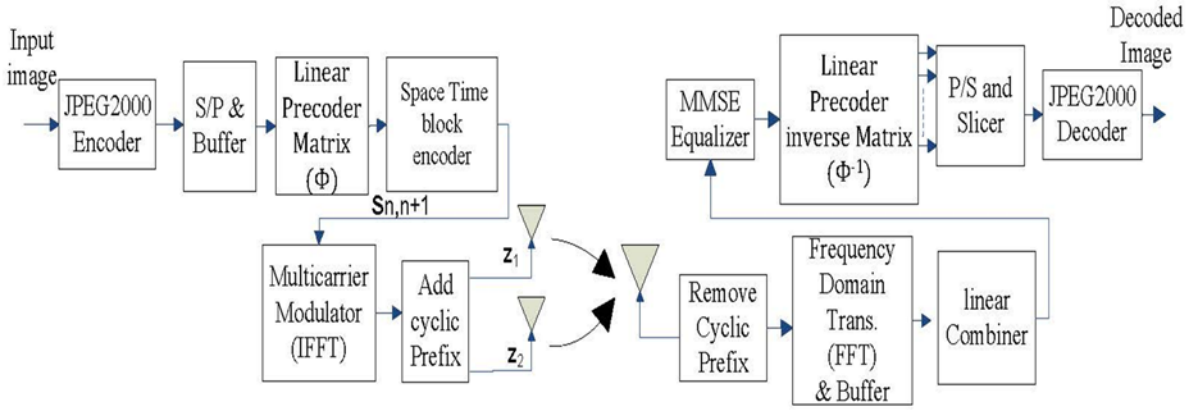

Figure 3-4: OFDM system model with EPA

for the sake of completeness. We assume that the channel is block fading frequency selective, and the CIR remains constant over the two time slots during which the space time block codes are transmitted. Section 3.1 has explained the transmission model for SCFDE system; in the following section the transmission model for LCP-OFDM system with two transmit antennas is discussed.

3.2.2. Orthogonal Frequency Domain Multiplexing Transmission Model

The OFDM system, initially, pre-codes the transmitting data with a linear constellation matrix to exploit multipath diversity. The resulting symbols are passed to the STBC block to generate different copies of the signal before the transmission. The output of the STBC block is depicted in Figure 3-2. Before the transmission, the OFDM transmitter

performs a Fourier transformation and sends the frequency domain symbols to the circulant structured channel in two different time slots.

$$\begin{aligned}\mathbf{r}_{n_1} &= \mathbf{H}_{n,1}\mathbf{Q}^H\boldsymbol{\theta}\mathbf{x}_{n,1} + \mathbf{H}_{n,2}\mathbf{Q}^H\boldsymbol{\theta}\mathbf{x}_{n,2} + \mathbf{v}_{n_1}\,,\\ \mathbf{r}_{n_2} &= -\mathbf{H}_{n,1}\mathbf{Q}^H\boldsymbol{\theta}\mathbf{x}^*_{n,2} + \mathbf{H}_{n,2}\mathbf{Q}^H\boldsymbol{\theta}\mathbf{x}^*_{n,1} + \mathbf{v}_{n_2}\,.\end{aligned} \tag{3-8}$$

In (3-8), $\mathbf{r}_{n_1}$ and $\mathbf{r}_{n_2}$ are the received signals at the receiver from the OFDM system in the first and the second time slot, respectively. $\mathbf{H}_{n,1}$ and $\mathbf{H}_{n,2}$ represent the circulant channel (structured in section 2.1) for the n^{th} transmission block from the first and second antenna, respectively. $\mathbf{x}_{n,1}$ and $\mathbf{x}_{n,2}$ denote the n^{th} block of transmitting data from the first and the second antenna, respectively. $\mathbf{v}_{n_1}$ and $\mathbf{v}_{n_2}$ are the AWGN vectors defined in Section 3.1.1. $\mathbf{Q}$ and $\boldsymbol{\theta}$ represent the FFT and the LCP matrices, respectively, both with the sizes of $N \times N$, where N is the number of subcarriers.

The receiver performs a serial to parallel conversion, discards the redundant cyclic prefix data, and executes a Fourier time domain transformation (i.e, multiplying by FFT matrix). Then, the receiver combines the received signals linearly, similar to (3-4). The resulting signals are concatenated into a single block, $\hat{\mathbf{r}}_n$. Then, the MMSE equalizer in (3-5) is used in the time domain, opposite to the SCFDE system which performs it in frequency domain. The output of the MMSE equalizer will be $\hat{\mathbf{y}}_n = \mathbf{W}_n\hat{\mathbf{r}}_n$. Afterward, the receiver compensates for the pre-coding in the transmitter by applying the inverse LCP matrix to recover the original data given by $\hat{\mathbf{x}}_n = \boldsymbol{\theta}^{-1}\hat{\mathbf{y}}_n$. At the end, a hard decision slicer is applied on the recovered data and passed to the JPEG2000 decoder to generate the received image.

3.3. Simulation Results

We develop our simulation results using Kakadu as the JPEG2000 image coder to encode image of Lena with a size of 512×512. We use BPSK as the modulation scheme for the codestream obtained from the codec, and assume that the header information is transmitted error free. Firstly, we analyze the performance of the UPA algorithm with SCFDE technique explained in Section 3.1. Secondly, we investigate trans-

mission of JPEG2000 images in the SCFDE and OFDM systems with equal power allocation, which has been explained in section 3.2.

3.3.1. Simulation Results Related to Section 3.1

Based on the previous experiments in [**9**], the value of α in (3-6) is set to be 0.01. The performance of the UPA algorithm with SCFDE technique is analyzed by calculating the PSNR of the received image transmitted through block fading frequency selective channels.

Figure 3-5 and Figure 3-6 present the PSNR performance of the single carrier system with multiple transmission antennas when combined with the UPA optimization algorithm for image transmission through frequency selective channels, at different channel taps. The benchmark in the PSNR performance evaluation in this section is the scenario in which the UPA algorithm is used alone for image transmission over block fading non-frequency selective channels. Figure 3-5 reveals a degradation in the PSNR of the received "Lena" when the number of channel taps increases. For example, at an SNR value of 10 dB, integration of UPA and SCFDE lowers the PSNR of the system in a 2-tap channel for about 6 dB in comparison with the single tap channel. The latter is also lowered by about 2.2 dB compared to the case where only UPA is used for transmission over frequency flat channels. Figure 3-6 illustrates similar trends in the PSNR profile of the received "Peppers". The reason for the lower PSNR performance at higher channel taps in the UPA-SCFDE system is that our UPA algorithm initially assumes an AWGN channel condition during the optimization process. To compensate for the channel fading, (3-6) is applied in the algorithm before the transmission. This equation eliminates the effect of the instantaneous channel fading; however, the SCFDE technique requires the multi-tap fading behavior of the channel to obtain multipath diversity and enhance the system performance as the number of channel taps increases.

Despite the loss in the PSNR profile at higher channel taps, our proposed system achieves spatial diversity when two transmit antennas are employed at the transmitter side and Alamouti's STBC is utilized. Figure 3-5 and Figure 3-6 demonstrate that at an SNR value of 10 dB, utilization of two transmitter antennas contributes to an increment of up to 2.5 dB in the PSNR of the received image transmitted through 2-tap frequency selective channel. Thus, we are able to receive the image with a higher quality at the re-

ceiver, or conserve energy by bounding the quality of the received image. Also at SNR values greater than 18 dB, the proposed system has a superior performance in a single tap channel in comparison to the benchmark scenario.

Figure 3-7 and Figure 3-8 present a visual comparison for transmission of "Lena" and “Peppers” (respectively) in the UPA-SCFDE system over the channel scenarios tabulated in Table 3-1. Note that the visual quality of the received image is enhanced when the number of transmitter antennas increases. In addition, increasing the number of channel taps lowers the quality of the received image.

Table 3-1: Transmission scenarios in the UPA-SCFDE system (SNR=16 dB)

Scenario	**Transmission Scenario**	**PSNR (dB)**	
		Lena	Peppers
(a)	Original Image	----	-------
(b)	Using UPA over non-frequency selective channel	27.99	27.22
(c)	Using UPA & SCFDE over 1-tap frequency selective channel with 2 transmission antenna	26.95	26.73
(d)	Using UPA& SCFDE over 1-tap frequency selective channel with 1 transmission antenna	24.95	24.32
(e)	Using UPA& SCFDE over 2-tap frequency selective channel with 2 transmission antenna	20.01	19.56
(f)	Using UPA& SCFDE over 2-tap frequency selective channel with 1 transmission antenna	17.15	15.57

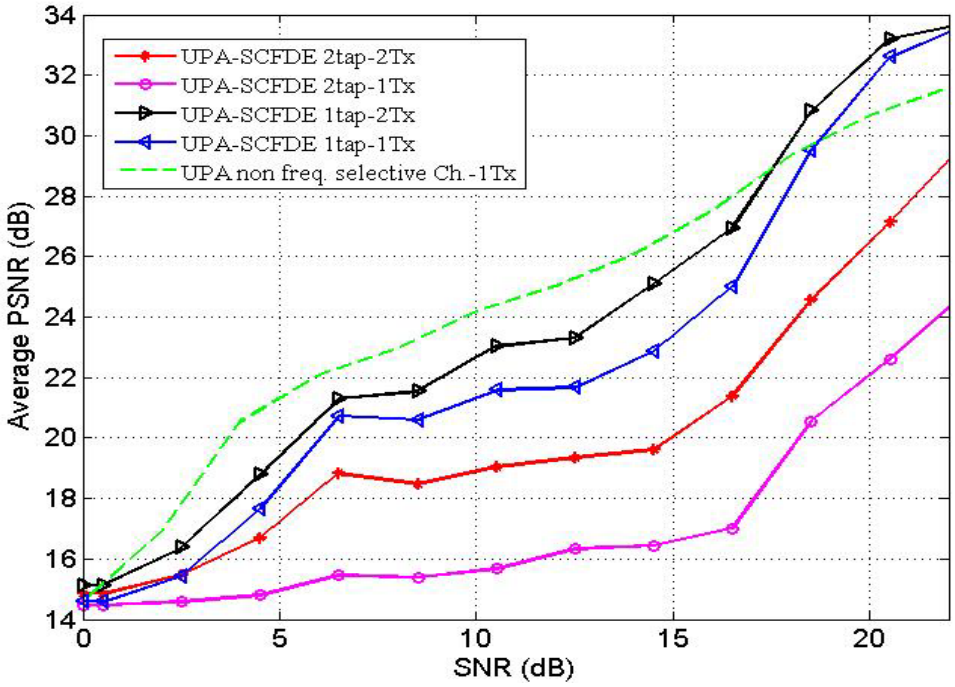

Figure 3-5: Comparison of the PSNR of the received Lena ($512 \times 512, 0.25$ bpp) in the UPA-SCFDE system

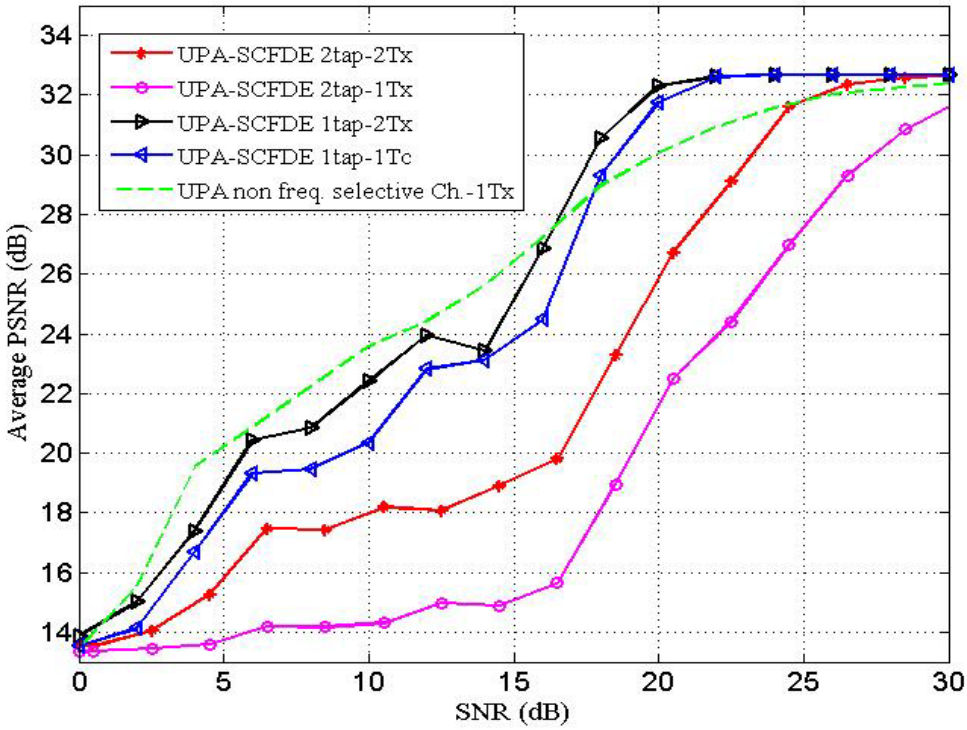

Figure 3-6: Comparison of the PSNR of the received Peppers ($512 \times 512, 0.25$ bpp) in the UPA-SCFDE system

(a) (b)

(c) (d)

(e) (f)

Figure 3-7: Visual comparison of "Lena" at 0.25 bpp, transmitted at SNR=16 dB over the scenarios in Table 3-1

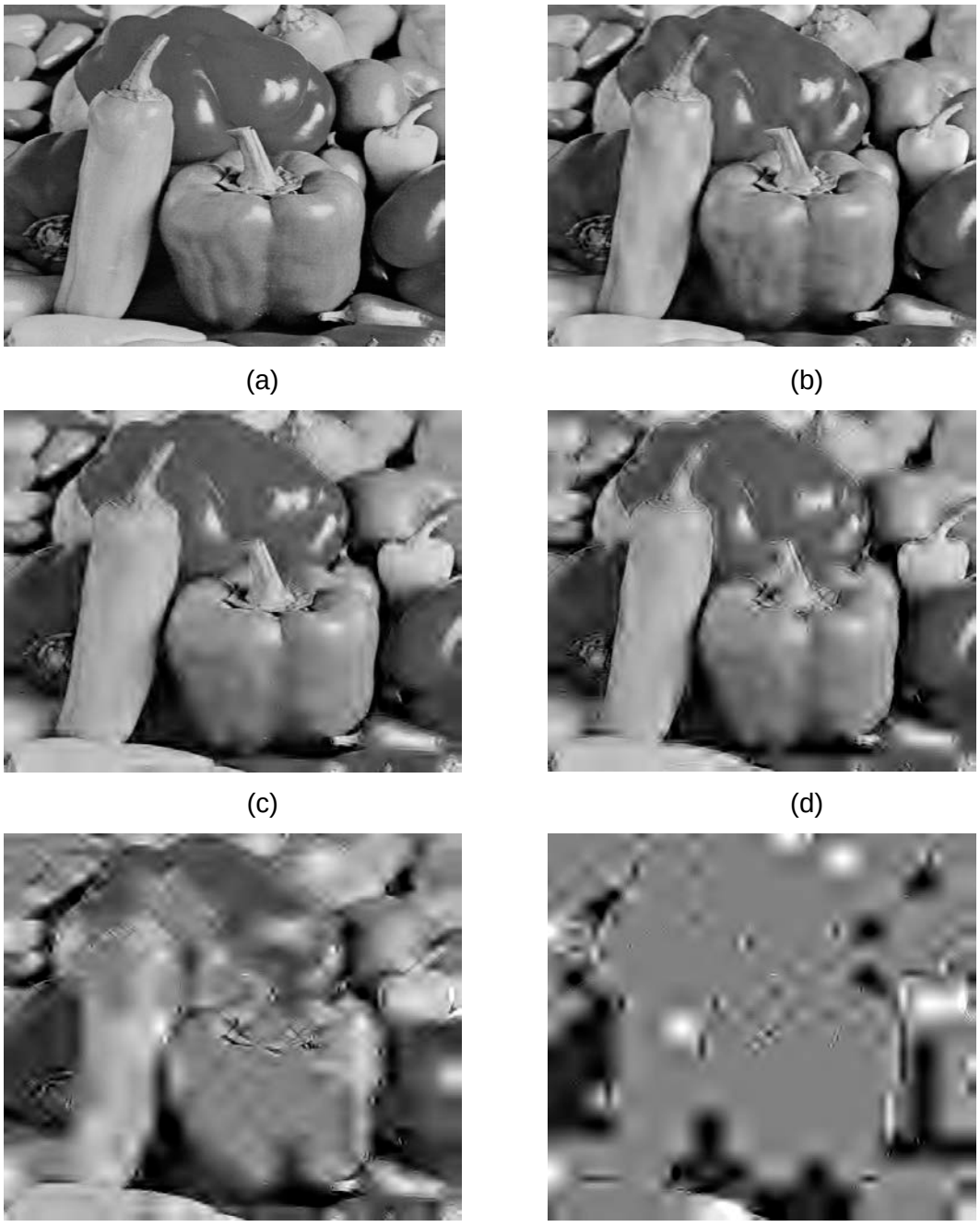

(a) (b)

(c) (d)

(e) (f)

Figure 3-8: Visual comparison of "Peppers" at 0.25 bpp, transmitted at SNR=16 dB over the scenarios in Table 3-1

3.3.2. Simulation Results Related to Section 3.2

We investigate the PSNR profile of the received image transmitted through block fading frequency selective channels, with different number of transmit antennas and for various source encoding rates.

In Figure 3-9, we compare the PSNR performance of the systems presented in Figure 3-3 and Figure 3-4, in a multi-tap channel and with one and two numbers of transmission antennas. The two systems present similar improvement trends in the case of 1-tap channel when the number of antennas is increased from one to two. In other words, both systems achieve spatial diversity with a gain of up to 10 dB, by employing two transmitter antennas and applying STBC to the transmitting codestream. For example, at an SNR value of 20 dB, the PSNR performance enhances up to 12 dB in a 1-tap channel when the number of transmitter antennas increases from one to two in the SCFDE and the OFDM systems. The OFDM system achieves a higher spatial diversity gain of up to 12 dB at an SNR value of 20 dB in a 2-tap channel condition, and this gain decreases to 5 dB for the SCFDE system. In addition, Figure 3-9 demonstrates that the higher is the number of channel taps in an OFDM system, the lower is the PSNR value of the received image. However, the SCFDE system exhibits an increase as high as 8 dB in the PSNR value of the received image when the number of channel taps increases from one to two. That is, in a severer channel condition, the SCFDE achieves multipath diversity, which leads to a better quality of the received image. This type of diversity, however, is not achievable in our OFDM system.

To achieve multipath diversity in an OFDM system as well, a linear constellation pre-coder is employed at the transmitter side. Figure 3-10 demonstrates that the LCP-OFDM system achieves multipath diversity. Note that the LCP-OFDM system has an improved PSNR performance even for 1-tap channel. As the number of channel taps increases to two, the LCP-OFDM improves the PSNR performance to a higher value than the OFDM does. Even though the LCP-OFDM system increases the PSNR value of the received image passed through a 2-tap channel, up to 3 dB at SNR value of 20 dB, yet it is not able to enhance the performance of a 2-tap channel over that of a 1-tap as the SCFDE does. However, at SNR values higher than 30 dB, the PSNR performance of the LCP-OFDM for a 2-tap channel converges to that of the 1-tap channel.

In Figure 3-11 and Figure 3-12, we evaluate the PSNR performance of the SCFDE and the OFDM system for different bit budgets, respectively. To establish a fair comparison between the two systems in this part, the images are transmitted only over a single tap channel to generate a PSNR profile without multipath diversity. The bit budget is varied for each SNR value by changing the average bits per pixel from 0.1 bpp to 0.3 bpp in steps of 0.05. For example at 0.1 bpp, the bit budget (i.e, the total number of bits of the codestream) is $21{,}000$ bits, and it increases to $73{,}120$ at 0.3 bpp. Thus, lowering the code rate is advantageous in conserving the bandwidth; however, it might deteriorate the image quality. Figure 3-11 illustrates that in our SCFDE system, at SNR values of less than 15 dB, the quality of the received image does not improve for higher coding rates. However, degradation of the received PSNR values at higher SNR values is notable when the coding rate decreases. Similar observations are valid when two transmitter antennas are utilized, except that we can conserve on bandwidth in this case by losing less of the quality in the received image. For example, when two transmitter antennas are used, we can save in bandwidth by lowering the coding rate from 0.3 bpp to 0.15 bpp, while keeping the PSNR of the received image above 30 dB -an acceptable quality for the received image- for SNR values higher than 30 dB. Figure 3-12 presents similar trend for the OFDM system when one and two antennas are utilized at the transmitter side. An interesting observation in Figure 3-11 (a) is that the PSNR performance at code rates between 0.1 bpp and 0.2 bpp outperforms the one at 0.25 bpp, when one transmitter antenna is used for SNR values between 10 dB and 20 dB. Depending on the application, insignificant loss in the quality can be sacrificed for the bandwidth conservation.

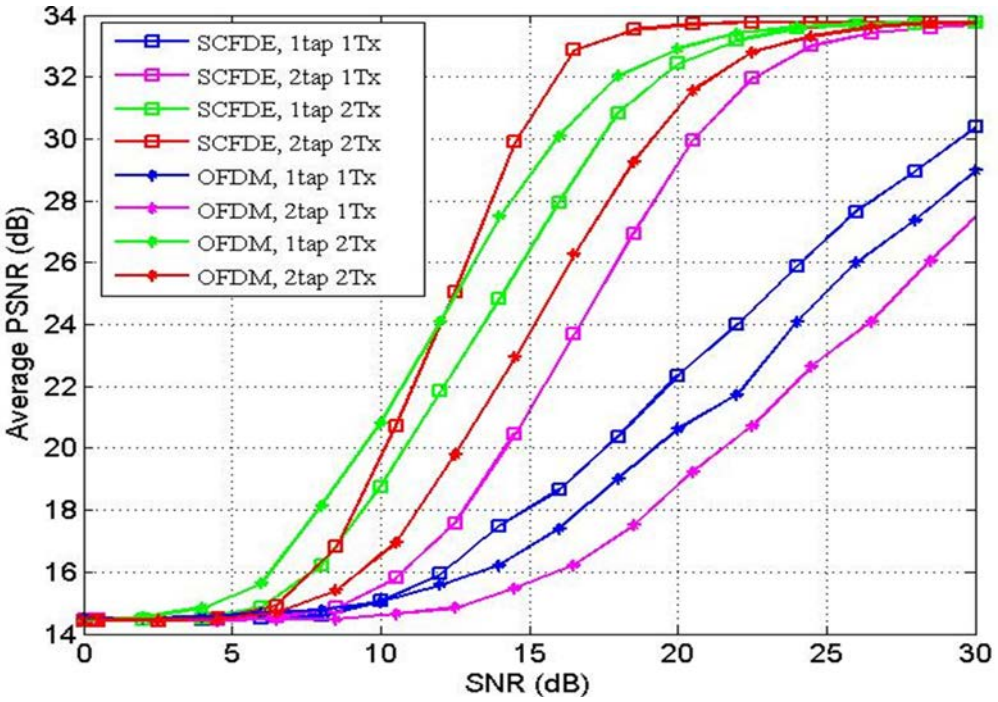

Figure 3-9: PSNR performance comparison of the received Lena ($512 \times 512, 0.25$ bpp) between SCFDE and OFDM systems with EPA

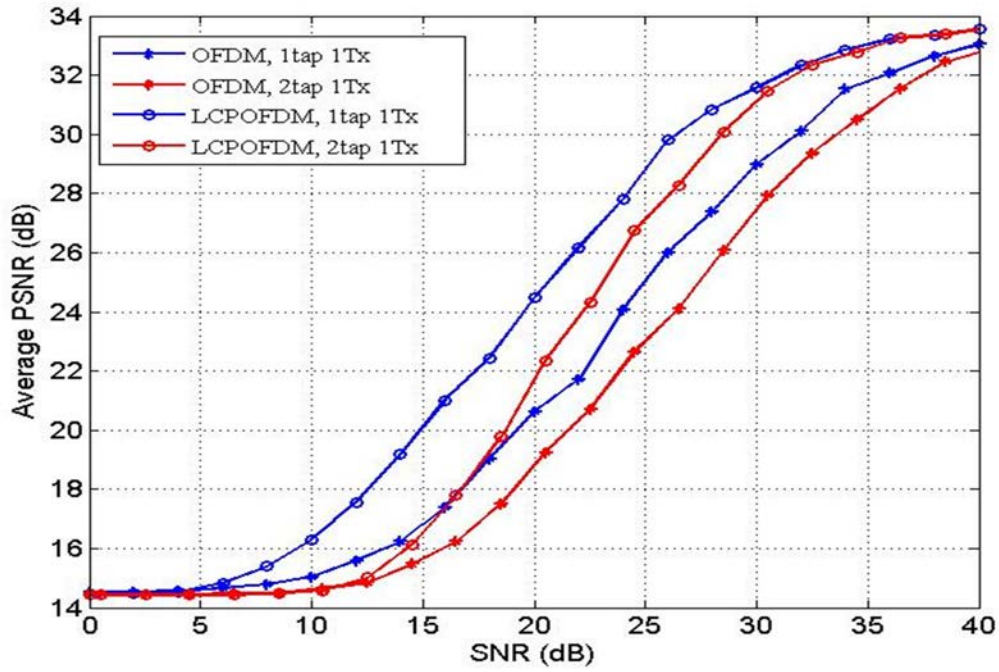

Figure 3-10: PSNR performance comparison of the received Lena ($512 \times 512, 0.25$ bpp) between OFDM and LCP-OFDM techniques with EPA

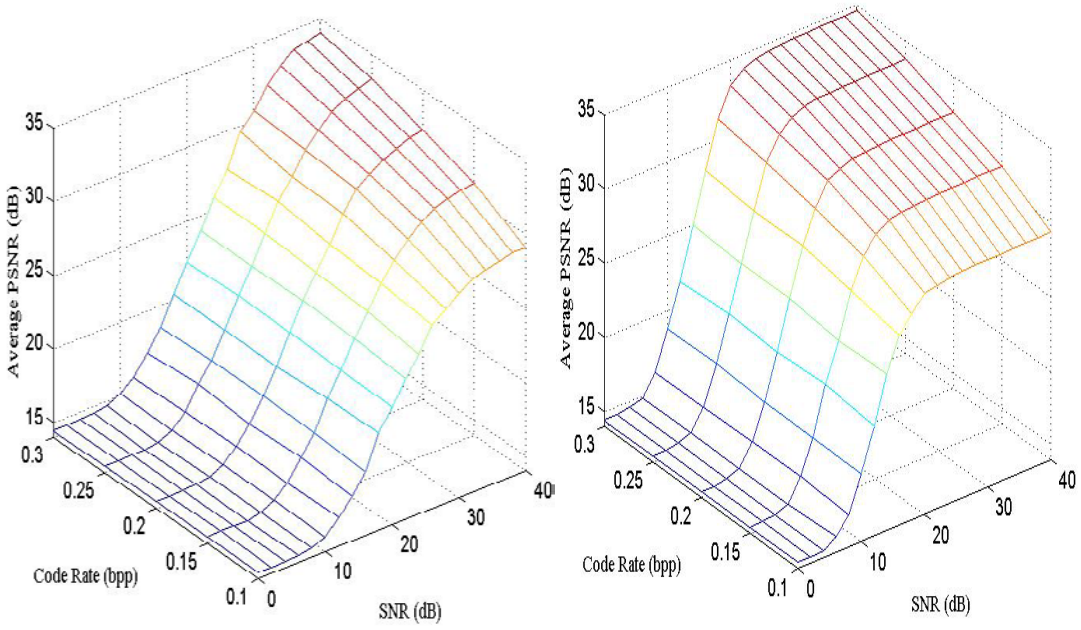

(a) (b)

Figure 3-11: PSNR performance comparison for different coding rates in EPA-SCFDE system (a) 1 transmitter antenna (b) 2 transmitter antennas

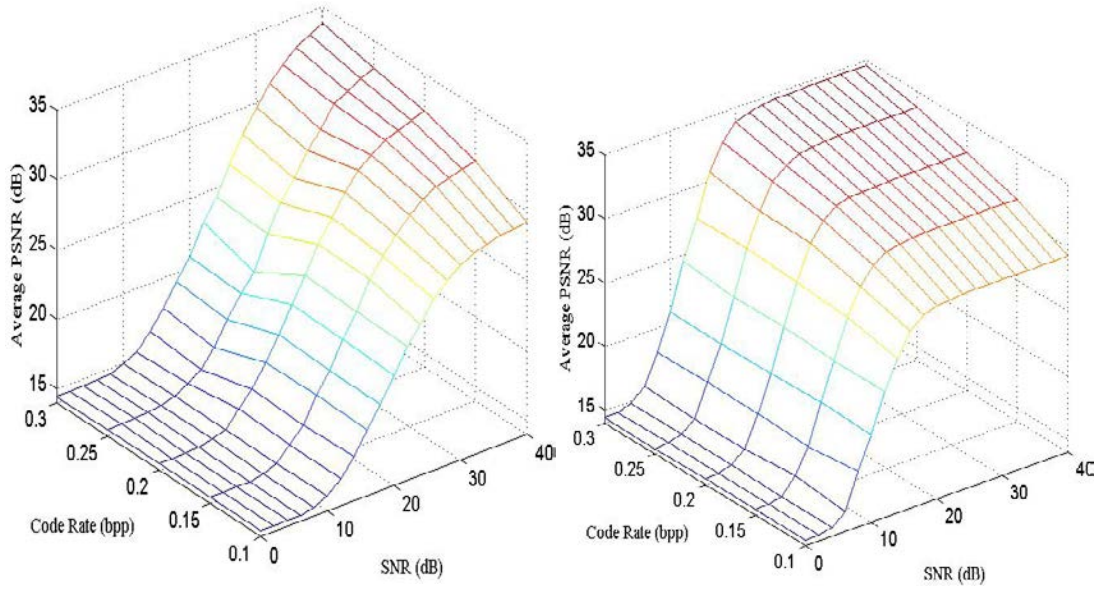

(a) (b)

Figure 3-12: PSNR performance comparison for different coding rates in the EPA-OFDM system (a) 1 transmitter antenna (b) 2 transmitter antennas

Reducing the coding rate not only saves the available bandwidth, but also reduces the file size and lowers the delay time in coding, transmitting, and decoding of the images. In medical applications, where seconds play important roles in survival, fast coding, transmitting, and decoding of an X-RAY or FMRI image is critical.

Figure 3-13 presents a visual comparison for transmission of "Lena" through block fading frequency selective channel with EPA over the scenarios tabulated in Table 3-2. To simplify the comparison, transmission through 1-tap channel is only considered. Note that the visual quality of the received image increases at higher number of transmission antennas. Similar visual quality of the received image at 0.15 bpp and 0.3 bpp, within the OFDM and the SCFDE systems for two transmitter antennas, implies that we can save in bandwidth by lowering bit budget without jeopardizing image quality.

Table 3-2: Comparison scenarios in between the SCFDE and the OFDM system with EPA (SNR=16 dB)for transmission of Lena

Scenario	**Transmission Scenario**	**PSNR (dB)**
(a)	Original image of Lena	------
(b)	Using OFDM, with 1 Transmitter antenna, at a rate of 0.3 bpp	18.48
(c)	Using SCFDE, with 1 Transmitter antenna, at a rate of 0.3 bpp	19.24
(d)	Using OFDM, with 2 Transmitter antenna, at a rate of 0.3 bpp	31.03
(e)	Using SCFDE, with 2 Transmitter antenna, at a rate of 0.3 bpp	28.62
(f)	Using OFDM, with 1 Transmitter antenna, at a rate of 0.15 bpp	18.21
(g)	Using SCFDE, with 1 Transmitter antenna, at a rate of 0.15 bpp	18.70
(h)	Using OFDM, with 2 Transmitter antenna, at a rate of 0.15 bpp	30.32
(i)	Using SCFDE, with 2 Transmitter antenna, at a rate of 0.15 bpp	27.45

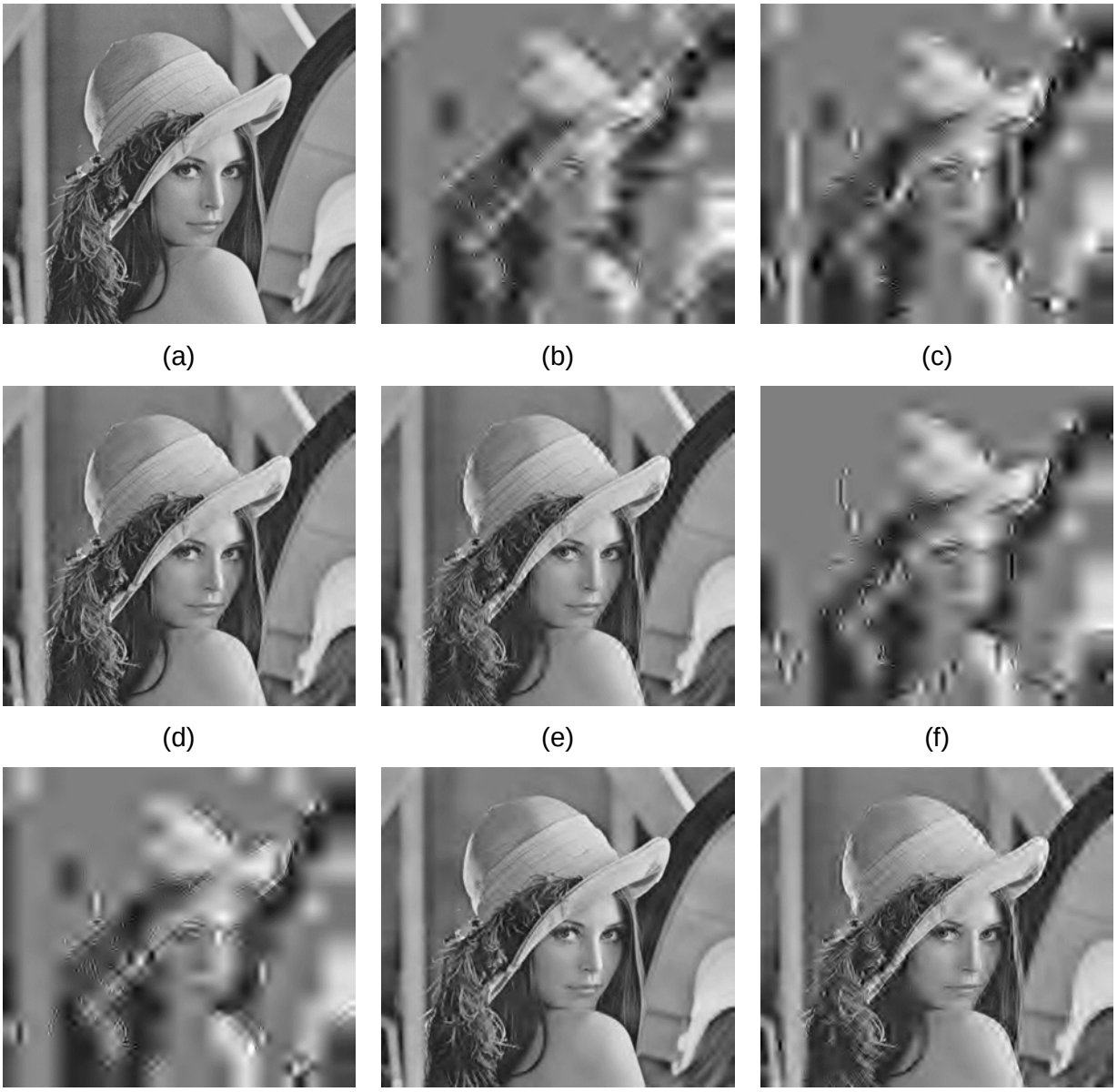

(a) (b) (c)

(d) (e) (f)

(g) (h) (i)

Figure 3-13: Visual comparison of "Lena", transmitted at SNR=16 dB over the scenarios in Table 3-2

3.4. Summary

Section 3.1 discusses transmission of JPEG2000 images through frequency selective block fading channels using an UPA algorithm and SCFDE technique. The optimization algorithm allocates unequal power to each coding pass based on its contribution to the quality of the received image. The simulation results for the image of Lena and Peppers demonstrate that even though the system is capable of combating the negative effects of ISI and ICI, but it cannot achieve multipath diversity. The simulation results prove the effectiveness of utilizing two transmission antennas and employing Alamouti's STBC diversity technique in enhancing the PSNR profile of the received image. For example, incrementing the number of channel taps from one to two in a single transmission antenna system leads up to 10 dB drop in the PSNR performance at an SNR value of 20 dB. However, in a two transmission antenna system, this degradation in the PSNR profile decreases to 6 dB. In addition, increasing the number of transmission antennas from one to two enhances the PSNR performance of the received images through 1-tap and 2-tap channel by about 0.5 dB and 4 dB, respectively, at an SNR value of 20 db. Comparing the PSNR profile of the UPA-SCFDE system in this chapter with the one of the UPA-OFDM system in Chapter 2 concludes that the latter system leads to a higher image quality than the former one.

Section 3.2 compares transmission of the JPEG2000 images transmitted through frequency selective block fading channels in multi-input single-output systems using SCFDE and OFDM techniques, with EPA. Spatial and multipath diversity are exploited by employing Alamouti's STBC and LCP techniques into our system design, respectively. The simulation results demonstrate that the SCFDE and the OFDM systems exhibit similar trend of improvement for single tap channel. However, the SCFDE system obtains multipath diversity and achieves a PSNR gain of up to 12 dB more than the OFDM system for a 2-tap channel. Employing the LCP technique improves the PSNR performance of the OFDM system in a 2-tap channel by 5 dB at an SNR value of 20 dB for the JPEG2000 images traversed through 2-tap channels. The results also illustrate that the systems achieve spatial diversity when STBC is integrated to the transmitter. The PSNR values increase up to 12 dB at SNR value of 20 dB when the number of transmitter antennas increase from one to two. Furthermore, the increase in the number of antennas bestows flexibility in saving the bandwidth by lowering the coding rate (consequently the

bit budget) without jeopardizing the PSNR performance. For example, at an SNR value of 30 dB with two transmitter antennas, we are able to save in bandwidth by lowering the coding rate down to 0.15 bpp, while the system maintains a PSNR performance of above 30 dB.

This chapter is the result of work published in [**37**].

4. Chapter 4: Conclusion and Future Directions

4.1. Summary and Conclusion

Transmission of still images over wireless channels with optimal protection techniques such as UEP or UPA techniques has attracted much attention in the field of multimedia communications. However, implementation of an UPA scheme over frequency selective channels requires an in-depth investigation of the received PSNR profile of an image for a range of SNR values, different channel memory lengths, multiple transmitter antennas, and various source coding rate.

In Chapter 2 of this thesis, we have proposed to integrate an UPA scheme with the OFDM technique to enable transmission of JPEG2000 images over frequency selective channels. We have validated the effectiveness of the UPA scheme in minimizing the total end to end distortion of the received images. Further, we have improved the UPA scheme by proposing an adaptive algorithm in which the code streams are categorized into variable length groups before the power allocation procedure. In addition, a channel assignment strategy is introduced to the system to transmit the more important coding passes over the subcarriers with higher gain. We have validated our results with extensive Monte Carlo simulations, and have evaluated them with competing schemes in the literature. The simulation results demonstrate the effectiveness of our OFDM based UPA system in maintaining the superior PSNR performance that the UPA system would yield without using the OFDM technique for non-frequency selective channel. In addition, the proposed adaptive scheme and the channel assignment strategy lead to a PSNR gain advantage when used in the OFDM transmitter of our system model.

In Chapter 3, we have proposed to integrate the UPA scheme with the SCFDE technique to enable transmission of the JPEG2000 images over frequency selective channels. Our system model incorporates the STBC technique to achieve spatial diversi-

ty, and we investigate the performance of the UPA algorithm in a multi-input single-output transmission system. The Monte Carlo based simulation results demonstrate the effectiveness of the SCFDE based UPA system in eliminating the negative impacts of ISI and ICI in a frequency selective channel. Even though the system achieves spatial diversity at higher number of transmitter antennas, but it suffers from loss of multipath diversity when the number of channel taps increases.

Also in Chapter 3, we have compared the performance of the OFDM and the SCFDE techniques for JPEG2000 image transmission over frequency selective channels, where the EPA technique is utilized. The comparison is based on measuring the PSNR values of the received images in a range of SNR values, with multi-tap channel condition, different number of transmitter antennas, and different source coding rates. The results demonstrate that both systems achieve spatial diversity; however, only the SCFDE obtains multipath diversity as the number of channel taps increases. To tackle this shortcoming of the OFDM system, we have introduced an LCP technique to the OFDM system. The simulation results present that the LCP-OFDM system achieves multipath diversity during the transmission of JPEG2000 images over frequency selective channel. In addition, the simulation results for the PSNR profile at different coding rates reveal that the SCFDE and the OFDM system can conserve bandwidth during transmission of JPEG2000 images, if lower bit budget is utilized and certain loss in the received image quality can be tolerated.

4.2. Future Work

Throughout this thesis, we have assumed a block fading frequency selective channel as the transmission medium for transmission of the JPEG2000 images. The followings are the possible directions for the extension of this research:

- **Evaluation of the UPA algorithm in a fast fading channel:**
  One possible direction to extend this work is to consider the fast fading behavior of a communication channel. In a fast fading channel, CSI is subject to rapid changes based on the coherence time of the channel. Because our UPA algorithm assumes that the CSI is available at the transmitter, effectiveness of this algorithm for different Doppler spread values of the channel should be determined.

- **Evaluation of the UPA algorithm in fading channel models other than the Rayleigh model**
  We have assumed the distribution model of the fading channel, throughout our research, to be Rayleigh fading distribution. However, other distribution models exist such as: Rician and Nakagami. One possible direction of extension to this research is to investigate the performance of the UPA algorithm in OFDM (and/or) SCFDE systems, with various types of distribution models for the wireless channel.
- **Extension of the UPA algorithm from JPEG200 still images into other still and motion picture standards**
  The UPA algorithm that we have utilized in this thesis was initially inspired for the JPEG2000 still images. Proving effectiveness of this algorithm for different standards of coding still images or video streams can be another direction of extension to this research.

References

[1] D. S. Taubman and M. W. Marcellin, *JPEG2000: Image Compression Fundamentals, Standards and practices*.: Kluwer Academic Publishers, 2002.

[2] F. Pancaldi et al., "Single-Carrier Frequency Domain Equalization," *IEEE Signal Processing Magazine*, vol. 25, no. 5, pp. 37-56, 2008.

[3] T. Acharya and P. S. Tsai, *JPEG2000 Standard for Image Compression: Concepts, Algorithems and VLSI Architecture*. New Jersey: John Wiley and Sons Incorporation, 2004.

[4] A. Natu and A. S. Taubman, "Unequal Protection of JPEG2000 Code-Streams in Wireless Channels," in *IEEE Global Telecommunications Conference (GLOBCOM)*, vol. 1, 2002, pp. 534-538.

[5] B. A. Banister, B. Belzer, and T. R. Fischer, "Robust Image Transmission using JPEG2000 and Turbo-codes," in *Proceedings of the 2000 International Conference on Image Processing (ICIP)*, 2004, pp. 375-378.

[6] N. Thomas, N. V. Boulgouris, and M. G. Strintzis, "Optimized Transmission of JPEG2000 Streams over Wireless Channels," *IEEE Transactions on Image Processing*, vol. 15, no. 1, pp. 54-67, 2006.

[7] Y. Wei, Z. Sahinoglu, and A. Vetro, "Energy Efficient JPEG2000 Image Transmission over Wireless Sensor Networks," in *IEEE Global Telecommunications Conference (GLOCOM)*, 2004, pp. 2738-2743.

[8] L. Atzori, "Transmission of JPEG2000 Images over Wireless Channels with Unequal Power Distribution," *IEEE Transactions on Consumer Electronics*, vol. 49, no. 4, pp. 883-888, 2003.

[9] M. Torki and A. Hajshirmohammadi, "Unequal Power Allocation for Transmission of JPEG2000 Images over Wireless Channels," in *IEEE Global Telecommunications Conference*, 2008, pp. 1-5.

[10] H. Houas, I. Fijalkow, and C. Baras, "Resource Allocation for the Transmission of Scalable Images on OFDM Systems," in *IEEE International Conference on Communications*, 2009, pp. 1-5.

[11] K. Munadi, M. Kurosaki, K. Nishikawa, and H. Kiya, "Error Protection for JPEG2000 Encoded Images and Its Evaluation Over OFDM Channel," in *Proceedings of the International Symposium on Circuits and Systems*, vol. 2, 2003, pp. 432-435.

[12] Y. Sun, Z. Xiong, and X. Wang, "Prospective Image Transmission over Differentially Space-Time Coded OFDM Systems: Research Articles," *Journal of Wireless Communications and Mobile Computing*, vol. 6, no. 8, pp. 1057-1075, December 2006.

[13] U. Sethakaset and S. Sumei, "Robust JPEG2000 Image Transmission over Closed-Loop MIMO-OFDM with Limited Feedback," in *IEEE International Symposuim on Personal, Indoor, and Mobile Radio Communications (PIMRC)*, 2008, pp. 1-5.

[14] C. Hsien Yun and C. Wei Ho, "Unequal Error Protection for OFDM Systems in Time-Varying Channels," in *Wireless Communications and Networking Conference (WCNC)*, 2011, pp. 1664-1669.

[15] H. Y. Chung and W. H. Chung, "Unequal Error Protection for OFDM Systems in Time-Varying Channels," in *IEEE Wireless Communications and Networking Conference*, 2011, pp. 1664-1669.

[16] Y. Qiao, Y. Wang, S. Yu, and D. Wang, "Robust Progressive Image Transmission Based on Multi-Rate Turbo Code and Space-Time OFDM," in *Proceedings of the Ninth International Symp. on Consumer Electronics*, 2005, pp. 128-133.

[17] M. M. Salah, A. A. Elrahman, and M. M. Mokhtar, "Performance Enhancement of Image transmission Using UEP Overlayed UTG_OFDM Scheme," in *National Radio Science Conference*, 2008, pp. 1-11.

[18] J. Song and K. J. R. Liu, "Robust Progressive Image Transmission Over OFDM Systems Using Space-Time Block Code," *IEEE Transactions on Multimedia*,

vol. 4, no. 3, pp. 394-406, September 2002.

[19] L. Toni, Y. S. Chan, P. C. Cosman, and L. B. Milstein, "Channel Coding for Progressive Image in a 2-D Time-Frequency OFDM Block with Channel Estimation Error," *IEEE Transactions on Image Processing*, vol. 18, no. 11, pp. 2476-2490, 2009.

[20] A. Elbehery, S. A. S. Abdelwahab, M. A. Elnabi, E. S. Hassan, and S. Elarabi, "Efficient Image Transmission Over the Single Carrier Frequency Division Multiple Access System Using Chaotic Interleaving," in *29th National Radio Science Conference (NRSC)*, 2012, pp. 411-420.

[21] H. S. Chu, B. S. Park, C. K. An, J. S. Kang, and H. G. Son, "Wireless Image Transmission based on Adaptive OFDM System," in *International Forum on Strategic Technologies (IFOST)*, 2007, pp. 623-626.

[22] S. Alamouti, "A Simple Transmit Diversity Technique for Wireless Communications," *IEEE Journal on Selected Areas in Communications*, vol. 16, no. 8, pp. 1451-1548, 1998.

[23] J. G. Proakis, *Digital Communications*. Boston: McGraw-Hill, 2000.

[24] A. H. Sayed, *Adaptive Filters*. Hoboken, New Jersey: John Wiley sons Inc., 2008.

[25] M. Torki, "JPEG2000 Transmission Over Wireless Channels Using Unequal Power Allocation," Engineering Science, Simon Fraser University, Burnaby, Canada, Master's Thesis 2009.

[26] N. Metropolis, A. W. Rosenbluth, M. N. Rosenbluth, A. H. Teller, and E. Teller, "Equation of State Calculations by Fast Computing Machines," *The Journal of Chemical Physics*, vol. 21, no. 6, pp. 1087-1092, June 1953.

[27] R. Negi and J. Cioffi, "Pilot Tone Selection for Channel Estimation in a Mobile OFDM System," *IEEE Transactions on Consumer Electronics*, vol. 44, no. 3, pp. 1112-1128, 1998.

[28] C. Shin, R. W. Heath, and E. J. Powers, "Blind Channel Estimation for MIMO-OFDM System," *IEEE Transactions on Vehicular Technologies*, vol. 56, no. 2, pp.

670-685, 2007.

[29] D. Dardari, M. G. Martini, M. Mazzotti, and M. Chiani, "Layered Video Transmission on Adaptive OFDM Wireless Systems," *EURASIP Journal on Applied Signal Processing*, vol. 4, no. 10, pp. 1557-1567, 2004.

[30] A. Sharma, S. De, and H. M. Gupta, "Energy-Efficient Transmission of DWT image over OFDM fading Channel," in *Third International Conference on Communication Systems and Networks (COMSNETS)*, 2001, pp. 1-7.

[31] M. Shayegannia, A. Hajshirmohammadi, S. Muhaidat, and M. Torki, "An OFDM Based System for Transmission of JPEG2000 Images Using Unequal Power Allocation," in *IEEE Wireless Communications and Networking Conference (WCNC)*, 2012, pp. 2064-2069.

[32] M. Shayegannia, A. Hajshirmohammadi, and S. Muhaidat, "Using an Adaptive UPA Scheme with a Channel-Aware OFDM Technique for Wireless Transmission of JPEG2000 Images," in *IEEE Canadian Conference on Electrical and Computer Engineering (CCECE)*, 2012.

[33] N. Al-Dhahir, "Single Carrier Frequency Domain Equalization for Space-Time Block-Codded Transmissions over Frequency-Selective Fading Channels," *IEEE Communications Letters*, vol. 5, no. 7, pp. 304-306, 2001.

[34] J. Yue and J. D. Gibson, "Performance of OFDM Systems with Space-Time Coding," in *IEEE Wireless Comm. and Networking Conference (WCNC)*, vol. 1, 2002, pp. 280-284.

[35] Z. Liu, Y. Xin, and G. B. Giannakis, "Linear Constellation Precoding for OFDM with Maximum Multipath Divesity and Coding Gains," *IEEE Transactions on Communications*, vol. 51, no. 3, pp. 416-427, 2003.

[36] Y. Xin, Z. Wang, and G. B. Giannakis, "Space-Time Diversity Systems Based on Linear Constellation Precoding," *IEEE Transactions on Wireless Communications*, vol. 2, no. 2, pp. 294-309, March 2003.

[37] M. Shayegannia, S. Muhaidat, and A. Hajshirmohammadi, "Transmission of JPEG2000 Images in an Uplink Cellular Network with UPA and SCFDE: A System Description," in *8th International Conference on Wireless and Mobile*

Communications, Venice, 2012.